



Can we reconstruct the formation of large open ocean polynyas in the Southern Ocean using ice core records?

Hugues Goosse¹, Quentin Dalaiden¹, Marie G.P. Cavitte¹, Liping Zhang^{2,3}

¹Earth and Life Institute, Université catholique de Louvain, Louvain-la-Neuve, Belgium

5 ²NOAA/Geophysical Fluid Dynamics Laboratory, Princeton, New Jersey, USA

³University Corporation for Atmospheric Research, Boulder, Colorado

Correspondence to: Hugues Goosse (hugues.goosse@uclouvain.be)

Abstract. Large open-ocean polynyas, defined as ice-free areas within the sea ice pack, have been observed only rarely over the past decades in the Southern Ocean. In addition to smaller recent events, an impressive sequence occurred in the Weddell
10 Sea in 1974, 1975 and 1976 with openings of more than 300,000 km² that lasted the full winter. Those big events have a huge impact on the sea ice cover, deep-water formation and more generally on the Southern Ocean and the Antarctic climate. However, we have no estimate of the frequency of the occurrence of such large open-ocean polynyas before the 1970s. Our goal here is to test if polynya activity could be reconstructed using continental records, and specifically, observations derived from ice cores. The fingerprint of big open-ocean polynyas is first described in reconstructions based on data from weather
15 stations, in ice cores for the 1970s and in climate models. It shows a clear signal, characterized by a surface air warming and increased precipitation in coastal regions adjacent to the eastern part of the Weddell Sea where several high-resolution ice cores have been collected. The signal of isotopic composition of precipitation is more ambiguous and we thus base our reconstructions on surface mass balance records only. A first reconstruction is obtained by performing a simple average of standardized records. Given the similarity between the observed signal and the one simulated in models, we also use data
20 assimilation to reconstruct past polynya activity. The impact of open ocean polynyas on the continent is not large enough compared to the changes due, for instance, to atmospheric variability to detect without ambiguity the polynya signal and additional observations would be required to discriminate clearly the years with and without open ocean polynya. It is thus reasonable to consider that, in these preliminary reconstructions, some high accumulation events may be wrongly interpreted as the consequence of polynya formation while some years with polynya formation may be missed. Nevertheless, our
25 reconstructions suggest that big open ocean polynyas, such as the ones that were observed in the 1970s, are rare events, occurring at most a few times per century. Century-scale changes in polynya activity are also likely but our reconstructions are unable to assess precisely this aspect at this stage.

1 Introduction

Polynyas are ice-free oceanic areas surrounded by sea ice. They are regularly observed close to the coasts of Antarctica where
30 very strong winds coming from the continent push the sea ice away from the shore as soon as it is formed (Comiso and Gordon,



1987; Morales Maqueda et al. 2004). The open ocean polynyas, which are polynyas that occur far from the coast, are rarer and thus much less known. Several short-lived open ocean polynyas have been observed in the Southern Ocean over the last decades, with relatively large ones in the Weddell Sea in 2016 and 2017 reaching 50,000 km² (Comiso and Gordon, 1996; Swart et al., 2018; Jena et al., 2019; Campbell et al., 2019). In addition to those relatively short-lived events, the great Weddell
35 Sea polynya (Fig. 1) of 1974, 1975 and 1976 was truly exceptional in historical records, first by its size of 300,000 km², i.e. about 10 times the size of Belgium, but also because it remained open all winter long (Carsey, 1980; Zwally et al., 1983).

In contrast to the coastal polynyas, wind alone is not sufficient to maintain open ocean polynyas. A major oceanic heat source is required to sustain the large heat loss at the atmosphere-ocean interface and prevent sea ice formation (Morales Maqueda et al., 2004). In the Weddell Sea, this is achieved by open ocean convection that continuously brings warmer water from the
40 deeper oceanic layers to the surface (Gordon, 1978; Martinson et al., 1981). For the Weddell polynya of the 1970s, oceanic observations indicate mixing to a depth of 3000 m compared to a depth of about 100 m in normal years (Gordon, 1982). During the formation of the polynya in 2017, the observed mixing reached a depth of more than 1700 m (Campbell et al., 2019).

Although the role of deep oceanic mixing appears crucial, the specific mechanisms leading to the formation of open ocean polynya in the Southern Ocean is still under debate. Compared to other regions of the world, the stability of the water column
45 is low in the Southern Ocean (Gordon and Huber, 1984; Martinson, 1990). The cold and relatively fresh surface water is separated from warmer water at depth by a relatively weak pycnocline. This warm deep water is supplied by an input from the Antarctic circumpolar current (the circumpolar deep water), which itself originates in the deep water formed in the North Atlantic. Nevertheless, the low stratification is maintained by strong sea ice-ocean feedbacks (Martinson, 1990; Goosse et al., 2018; Wilson et al., 2019) and open convection reaching large depths is very rare.

50 The opening of a polynya is triggered by the winds and specifically by the passage of storms that export sea ice out of the region, enhance turbulent mixing in the ocean and may bring additional heat (Morales Maqueda et al., 2004; Cheon et al., 2015; Jena et al., 2019; Francis et al., 2019; Campbell et al., 2019). After the formation of the polynya by a particular event, the convection is self-sustained. The warmer, saltier waters at depth are strongly cooled when they reach the surface by direct exchanges with the atmosphere, become denser and sink again to great depths.

55 In addition to the triggering by a perturbation, deep convection requires some preconditioning of the ocean, reducing the overall stability of the water column. This can be due to the build-up of a large heat reservoir at depth or to a reduced freshwater input at surface. Changes in surface winds also influence the horizontal oceanic circulation, potentially inducing upwelling of deep waters and thus a salt input in the surface layers creating conditions more prone to deep convection (Cheon et al., 2015; Campbell et al., 2019; Kaufman et al., 2020). In this framework, it has been argued that a persistent negative phase of the
60 Southern Annular Mode (which is the main mode of atmospheric variability in the Southern Hemisphere extra-tropics) in the preceding decade could have created favorable conditions for the formation of the Weddell polynya in the 1970s (Gordon et al., 2007; Kaufman et al., 2020). Finally, the convection itself provides a preconditioning for subsequent years as it maintains a low stability of the water column, explaining why open ocean convection and polynya formation can be sustained over



several years. The deep convection shuts down due to freshwater input at the surface, if the warm water at depth becomes too
65 cold to prevent the formation of sea ice even if it reaches the surface, or if storms during a particular year are too weak to
trigger the convection (Comiso and Gordon, 1987; Campbell et al., 2019).

The great Weddell Sea polynya of the 1970s originated in the region close to a seamount called Maud Rise (at about 3°E,
64°S). This region is considered as particularly prone to polynya formation and short-lived polynyas are often observed there
70 (Comiso and Gordon, 1996; Morales Maqueda et al., 2004). The main reason comes from interactions between the topography
and the large scale circulation that lead to a shallowing of the mixed layer, upwelling of warmer deep water and generation of
mesoscale oceanic eddies inducing an overall reduced stability of the water column (Carsey, 1980; Comiso and Gordon, 1987;
Holland, 2001; Kurtakoti et al., 2018). The influence of oceanic mesoscale eddies is not limited to the triggering of polynyas
as it has been suggested that interactions between the mean circulation and the formation of eddies plays an important role in
the generation of open ocean convection (Le Bars et al., 2016; Jüling et al., 2018). Eddies could also be a key element in the
75 preconditioning of the water column and in ocean restratification leading to polynya termination (Dufour et al., 2017; Weijer
et al., 2017).

The great Weddell Sea polynya of the 1970s had a large impact on the ocean state. The heat loss has been estimated to be of
the order of $0.4 \cdot 10^{21} \text{ J year}^{-1}$ (Gordon, 1982). This corresponds to 4% of the heat stored in the ocean in response to human-
induced perturbations in recent years (about $1 \cdot 10^{22} \text{ J year}^{-1}$, Lyman and Johnson, 2014; Resplandy et al., 2018). Furthermore,
80 the deep convection occurring in polynyas can lead to the formation of Antarctic Bottom Water (AABW). AABW is a key
water mass, present over the majority of the ocean floor, and occupies more than 30 % of the global ocean volume (Mantyla
and Reid, 1983; Johnson, 2008). It has its main origin at the margin of the Antarctic continent when cold and salty waters,
formed on the Antarctic continental shelves because of brine rejection during sea ice formation, sink to great depths (Foster
and Carmack, 1976; Purkey et al., 2018). During the polynya years in the 1970s, the volume of surface water entrained at
85 depth in the Weddell Sea was higher than along the continental margin (Gordon, 1982) but the overall contribution of deep
convection in AABW formation is highly uncertain (Martinson et al., 1981; Gordon 1982). Open ocean convection also
influences horizontal oceanic circulation, in particular the strength of the Antarctic Circumpolar current and of the subpolar
gyres (Behrens et al., 2016).

As the deep convection induces a large cooling at depth, a warming is expected to follow the event and 10% of the warming
90 observed at the bottom of the ocean over the last decades may be due to recovery from the consequences of the great Weddell
Sea polynya during the 1970s (Robertson et al., 2002; Zanowski et al., 2015). It has also been suggested that many changes
observed recently in the Southern Ocean are related to the occurrence of the Weddell Sea polynya 40 years ago (Zhang et al.,
2019). In particular, the perturbation induced by the polynya formation may have been able to overwhelm the response of the
Southern Ocean to the increase in greenhouse gas concentrations and might explain the discrepancies between many climate
95 model results and observations over the last decades (Latif et al., 2013; Zhang et al., 2019).



The direct contact between the ocean at a temperature close to its freezing point and the very cold air above in open ocean polynyas in the winter has significant impacts on the atmosphere. The large turbulent fluxes induce an increase of the air temperature over the polynya area that can lead to a 20 degrees warming in winter compared to non-polynya years (Moore et al., 2002). The enhanced evaporation over the polynya leads to a higher moisture content of the air, more clouds and more precipitation locally (Carsey, 1980; Moore et al., 2002; Weijer et al., 2017). The surface conditions may also induce a decrease of sea level pressure over the polynya and thus influence the atmospheric circulation (Timmermann et al., 1999; Moore et al., 2002; Latif et al., 2013; Weijer et al., 2017; Kaufman et al., 2020).

The local anomaly created over the polynya is transported downwind (e.g., Weijer et al., 2017), influencing the oceanic regions outside the polynya area, as well as the Antarctic continent. However, the signal there is less strong than over the polynya region and it is generally difficult to identify the effect of the polynya within the natural variability of the climate system (Carsey, 1980; Moore et al., 2002; Weijer et al. 2017).

Climate models have relatively large biases in their representation of vertical exchanges and deep water formation in the Southern Ocean (Heuzé et al., 2013; Sallée et al., 2013). Furthermore, widespread open ocean convection occurs nearly every year in some models (Manabe et al., 1991; Goosse and Fichefet, 2001; Stössel and Kim, 2001; Heuzé et al., 2013) while other models have limited or no open ocean convection. It may be tempting to consider that they have a more adequate representation of the Southern Ocean circulation than the ones that strongly overestimate it, as open ocean convection has rarely been observed in the past decades. However, it is not currently clear whether models without open convection lack an important mode of deep water formation or only a process of marginal importance that can be neglected (de Lavergne et al., 2014; Purkey et al., 2018; Kerr et al., 2018).

Finally, a few models display intermittent open ocean convection that leads to the formation of polynyas covering a wide range of sizes and duration (Martin et al., 2013; Stössel et al., 2015; Zanowski et al., 2015; Weijer et al., 2017; Zhang et al., 2019; Kaufman et al., 2020). The opening of those polynyas seems to be generally related to a common mechanism, implying a slow warming at depth due to the input of warmer water originating from the north when convection is shut down, followed by a rapid cooling at depth and surface warming during years with open ocean convection.

Unfortunately, the short instrumental records do not provide precise estimations of the frequency and the overall role of polynya formation and deep convection in the climate system nor can they be used to determine which climate models represent polynya occurrence adequately. It has been suggested that open ocean convection was more widespread in the past, with a reduction over the last decades that may have been caused by the large scale freshening observed in the Southern Ocean (de Lavergne et al. 2014). Human-induced climate change will likely reduce further the probability of ocean convection in the future (de Lavergne et al., 2014; Heuzé et al., 2015). However, it is difficult to assess the magnitude of any recent change in polynya occurrence and their impact.

An option is then to study a time period longer than the one covered by instrumental observations and rely on the signal stored in natural archives. Unfortunately, to our knowledge, no high-resolution ocean sediment core that might provide a direct record



of polynya activity is available and, up to now, no reconstruction of polynya occurrence has been developed for the past
130 centuries. This implies that the frequency of open ocean polynya formation is basically unknown.

However, even though no high-resolution paleoclimate data is available in the oceanic region where the signal due to polynyas
is the largest, polynyas have an influence on the continent too and it might be possible to reconstruct their occurrence from a
network of continental records. In that framework, ice core records are likely the best candidate as they provide high resolution,
well-dated records of climate changes over the Antarctic continent.

135 Our goal here is to test if it is possible to reconstruct polynya activity using available ice core records, in particular the water
isotopic composition ($\delta^{18}\text{O}$) and surface mass balance for which recent compilations have been developed (Stenni et al., 2017a;
Thomas et al., 2017). The first step is to estimate, using modern observations and model results, where the signal is likely to
be the clearest over the continent. This is done in section 3. To leave an imprint in a natural archive, which generally has an
annual resolution at best, the polynya must be large enough and stay open for a sufficiently long time. We thus focus on the
140 major events such as the great Weddell polynya observed in 1974, 1975 and 1976. In section 4, we then determine how the ice
core data can constrain the evolution of polynyas over the past centuries using a very simple statistical technique and data
assimilation.

2 Data and methods

2.1 Observations

145 To characterize the continental temperature changes occurring during the opening of the great Weddell polynya in 1974, 1975
and 1976, we will first use direct observations from weather stations as well as a spatial reconstruction of temperatures based
on these observations covering the period 1958-2012 (Turner et al., 2004; Nicolas and Bromwich, 2014a).

Measuring precipitation directly in Antarctica is much more difficult than temperature and many weather station records do
not include this variable routinely (Turner et al., 2004). We will thus rely on a recent synthesis of surface mass balance (SMB)
150 from 79 ice cores (Thomas et al., 2017). The surface mass balance is defined as the net surface accumulation resulting from
precipitation minus removal from snow drift and sublimation, but it is mainly influenced by snow falls over Antarctica (e.g.
Lenaerts et al., 2019). The ice core data provide direct but point estimates at the core locations. Additional information on the
spatial structure of the changes during polynya formation can be obtained from a reconstruction of the surface mass balance
(Medley and Thomas, 2019) that combines ice core data and atmospheric reanalysis fields in order to cover the whole grounded
155 Antarctic ice sheet over the past 200 years. This combination has the advantage of using the spatial covariance represented in
the reanalysis without the potential troubles associated with the lower quality of the reanalyses before 1979 and the
inhomogeneities associated to the inclusion of additional satellite observations after that date (Marshall, 2003; Nicolas and
Bromwich, 2014a).



In addition to the characterization of the changes occurring in the 1970s, the SMB records will be one of the main sources for
160 our reconstruction of polynya activity over the past centuries. The other data set is a synthesis of isotopic variations ($\delta^{18}\text{O}$)
including 112 cores (Stenni et al., 2017a). SMB and $\delta^{18}\text{O}$ are the two variables measured in ice cores selected here because
they are used routinely to interpret past changes in precipitation and temperature over Antarctica. Furthermore, the syntheses
available (Stenni et al., 2017a; Thomas et al., 2017) provide a reasonably good coverage over Antarctica, in particular in the
South Atlantic sector where we expect the strongest signature of the great Weddell Sea polynya formation. Several model-data
165 comparisons have also been carried out using those variables (e.g., Klein et al., 2019; Dalaiden et al., 2020), which therefore
provide a basis for the reconstructions using data assimilation described here.

Stenni et al. (2017a) and Thomas et al. (2017) selected only ice cores with a good time resolution and a low dating uncertainty.
The dating error is thus small for the cores included in these syntheses with a maximum of a few years over the past centuries.
This is essential for polynya detection since a sequence of opening may only last a few years. Here, we will be even more strict
170 and select only a subset of those data with annual resolution and the lowest age uncertainty, following the choice of Medley
and Thomas (2019) (see Table 1).

It may be difficult to make the distinction from available records between a year characterized by a few exceptional
precipitation events such as atmospheric rivers that leave a large imprint on surface mass balance (e.g., Gorodetskaya et al.,
2014; Turner et al., 2019) and the consequences of the opening of a polynya. As the focus here is on large open ocean polynyas
175 that are assumed to occur in sequence of several years, a 3-year running mean is applied on the time series in the majority of
our analysis. This provides a good balance between smoothing atmospheric events that may dominate at the interannual
timescale while still being able to identify polynya sequences lasting a few years as the one between 1974 and 1976. We also
remove the trend over the period 1850-1992 in the ice core records. Those trends are due to a large extent to processes unrelated
to polynya formation (Medley et al., 2018; Medley and Thomas, 2019). A part of the trend could be due to a recent shift in
180 polynya activity (e.g., de Lavergne et al., 2014) but it is impossible to disentangle at this stage the various contributions. We
thus preferred to remove the trend to avoid misinterpretations. After detrending, we ensure that the mean of the ice core records
before 1850 is the same as after 1850. This assumes a stationarity of the time series. Unfortunately, this procedure forbids us
to compare the frequency of open ocean polynya formation during the 20th century with previous periods.

2.2 Model results

185 From a description of the observed temperature and precipitation changes in 1974, 1975 and 1976, it is impossible to
disentangle the impact of polynya formation from the variability of the system that is not connected to the polynya itself.
Observations are thus complemented by the results of model simulations. The first simulation was performed with the
atmospheric model ECHAM5-wiso (Steiger et al., 2017; 2018) driven by observed changes in sea surface temperature and sea
ice concentration from the Met Office Hadley Centre's sea ice and sea surface temperature data set over the period 1871 to
190 2011 (Rayner et al., 2003 and updates). ECHAM5-wiso has a spatial resolution of 1.125° and simulates explicitly the water



isotopes. It provides thus a direct estimate of the model response in terms of temperature, SMB and $\delta^{18}\text{O}$ over Antarctica to observed changes in ocean surface conditions in 1974, 1975 and 1976.

Several climate models display polynyas of various sizes and locations. Because of the triggering effect of Maud rise, it is likely that, if large polynyas occurred in the Weddell Sea before the 1970s, they were also located close to the ones observed in the 1970s. Nevertheless, assessing the realism of simulated polynyas is difficult as we do not know if the sequence observed in the 1970s corresponds to the standard size of polynya we should expect in the current climate, if they were among the largest ones observed during the past centuries or if much bigger ones occurred earlier.

Here, two control simulations performed with the SPEAR (Seamless system for Prediction and Earth system Research) global climate model (Delworth et al., 2020), developed at the Geophysical Fluid Dynamics Laboratory are chosen because they display intermittent polynya formation whose size and characteristics share many elements with observed changes in the Southern Ocean (Zhang et al., 2019; Zhang et al., 2020). They have constant forcing and are not constrained by any observations. They could thus not reproduce the observed conditions in the 1970s but they provide a large number of events and thus a robust attribution of the impact of modelled polynya on the Antarctic continent. Furthermore, these simulation results provide the model prior in the data assimilation, as explained below. It is thus important to assess their characteristics compared to observations.

The two SPEAR simulations use the same ocean model, MOM6, with the SIS2 sea ice component (Adcroft et al., 2019), at a horizontal resolution of about 0.5° in the Southern Ocean. The first simulation, referred hereafter to as SPEAR_LO, includes the AM4 atmospheric component (Zhao et al., 2018) at a resolution of about 100 km. The second, SPEAR_AM2, uses AM2 (Anderson et al., 2004), an earlier version of the model at a resolution of about 200 km (see Zhang et al., 2020 for a longer description of the differences between the two simulations). For both simulations, we analyze here the last 1000 years of the experiments, corresponding to years 2000-3000 in SPEAR_AM2 and years 3000-4000 in SPEAR_LO.

2.3 Reconstruction methods

For reasons explained in Sect. 4, we have only selected the surface mass balance records for our reconstructions. The occurrence of polynyas over the past centuries is first estimated using a simple and direct method that will be described in the same section. Additionally, the history of past polynya formation is derived using data assimilation, a technique that has been applied recently to reconstruct climate fields, such as surface temperature and variables related to hydrology, over the past millennium (e.g., Goosse et al., 2012; Hakim et al., 2016; Franke et al., 2017; Steiger et al., 2018). Here, we apply the so-called offline or non-cycling data assimilation as in many previous studies (e.g., Hakim et al., 2016; Franke et al., 2017; Steiger et al., 2018; Klein et al., 2019), meaning that it is based on an existing ensemble and no additional simulation is performed in contrast to online data assimilation.

The technique is based on a particle filter, following the implementation of Dubinkina and Goosse (2013) (see also Klein et al., 2019 and Dalaiden et al., 2020). An ensemble of states is first obtained from the existing simulations, here the different



years of the control runs of SPEAR_AM2 or SPEAR_LO, which form the prior. The likelihood of each of these states for every year of the reconstruction is then evaluated from the differences between the model results and observations. On this basis, a weight is given to each model state as a function of this likelihood. This provides the posterior distribution from which we can, for instance, obtain the mean reconstruction as a weighted mean of the ensemble members. This technique in theory allows to reconstruct any variable that is simulated by the model and thus here the occurrence of polynyas.

In our experiments with data assimilation, the records are averaged over $\sim 500 \times 500$ km boxes, as coarse resolution models are not expected to correctly represent smaller scales. These averages is shifted by a constant value and scaled to have the same mean and variance as the reconstruction of Medley and Thomas (2019) for the same boxes over the period 1941-1990. The surface mass balance has a large spatial variability at all spatial scales (Thomas et al., 2017; Laepple et al., 2019; Cavitte et al., 2020) and this procedure provides values that are not too sensitive to the mean conditions at specific locations. Technically, this can be considered in the present framework as part of the observation operator that allows the correspondence between model space and observation space.

A key element in data assimilation is to obtain a reliable estimate of the observation error. As classically done, we consider that the errors are not correlated and that the observation error covariance matrix is diagonal. Because of the large spatial variability mentioned above, we also assume here that the representation error is much larger than the measurement error (Thomas et al., 2017; Laepple et al., 2019; Cavitte et al., 2020; Badgeley et al., 2020) and we only include the contribution of the former in our estimate of the error. The representation error is due in particular to the fact that the model is not able to simulate the small-scale processes that are included in the signal recorded in the archive (the so-called ‘error of representation due to unresolved scales and processes’, see for instance Janjić et al., 2018). The representation error is estimated by using a high resolution (approximately 27 km) simulation performed with the regional atmospheric model RACMO over the period 1979-2016 (van Wessem et al., 2018). It is obtained by calculating the standard deviation of the difference between the average of the annual mean surface mass balance time series using only the RACMO grid boxes where ice core records are available and the true average over the continental part of the 500 by 500 km boxes. The mean of all the simulated series over the period 1976-2016 is removed before the standard deviation is calculated to focus on the time variability within the boxes, not on the differences in mean accumulation. This standard deviation is then multiplied by a factor 0.6 to take into account the smoothing associated to the 3-year running mean applied to the time series (see above). We prefer this method over than computing directly the standard deviation after applying a 3-year running mean on the time series of simulated results because of the small number of samples in the RACMO simulation.

3 Fingerprint of polynyas in observation and models

The annual mean temperature in the reconstruction of Nicolas and Bromwich (2014a) shows a large and clear positive anomaly over years 1974-1976 in continental regions located close to the eastern Weddell Sea where the large polynyas appear in the 1970s. Specifically, higher temperatures are found between 50°W and the Greenwich Meridian, with a maximum reaching



255 more than 2°C near the coast (Fig. 2a). The number of weather stations being low in Antarctica, this positive temperature anomaly is mainly influenced by observations at the Halley station, which is located at 75.6°S, 26.6°W and is the weather station that is the closest to the great Weddell Sea polynya (Carsey, 1980). The other weather station with a long record in the region is Novolazarevskaya (70.8°S 11.8°E) which, by contrast, does not display particularly warm conditions at that time (Fig. 2b).

260 Halley station shows multidecadal variability with generally higher temperatures between 1970 and 1990 than in the following two decades. When applying a 3-year running mean to smooth interannual variability while keeping the signal associated to the observations of polynyas three year in a row, the maximum of the whole series is reached in 1976, i.e. during the polynya formation period. However, the annual mean temperature anomaly compared to the period 1958-2000, with a value of 1.6°C, does not appear exceptional or out of the normal range of variability for the region (standard deviation of the annual mean

265 temperature is 0.7°C). Furthermore, when taking a 3-year period, the maximum at Halley is not for the polynya years 1974-1976 but is shifted by one year (1975-1977). This may be due to the drift of the polynya toward the west from 1974 to 1976, moving closer to Halley Station in the final years (Carsey, 1980; Zwally et al., 1983). Furthermore, we analyze here annual mean temperatures. The late freezing or the early melting of the sea ice in years preceding or following the polynya created large embayments but not strictly polynyas (Carsey, 1980; Zwally et al., 1983). The effect of the polynyas on annual mean

270 temperatures can thus be extended in time even though no polynya strictly-speaking is formed in winter during those years. Snow accumulation is also higher in 1974-1976 in the continental regions close to the polynya (Fig. 3a). The signal appears more spatially extensive in the SMB reconstruction of Medley and Thomas (2019) than for temperature in the Nicolas and Bromwich (2014a) reconstruction, with positive values over nearly half of the continent. However, it is unlikely that they are all related to the great Weddell Sea polynya formation.

275 The integrated surface mass balance over the continental region close to the polynya, defined here as the domain between 50°W and 0°E northward of 80°S (see the sector indicated on Fig. 3a), has a local maximum in 1975 after applying a 3-year running mean (Fig. 3b). This corresponds exactly to the 3-year period with polynya formation but, as for temperature, the maximum does not particularly stand out in the time series and is, for instance, slightly lower than the one in 1995 when no major polynya was observed. In this region, the accumulation averaged over 1974-1976 is 12 Gt/y higher than the mean over the period 1958-

280 2000. If a slightly larger domain covering 50°W-50°E is considered, a value of 24 Gt/y is obtained and 1975 is the absolute maximum over the period 1958-2000. Those numbers can be compared to a standard deviation of the SMB in those regions of 7 and 15Gt/y, respectively, and a standard deviation at the scale of Antarctica of 57 Gt/y over the period 1958-2000 in the Medley and Thomas (2019) reconstruction after applying a 3-year running mean.

The temperature signal in the ECHAM5-wiso simulation driven by observed sea surface temperature and ice concentration is

285 very strong in the polynya region, with a warming reaching 2.5°C averaged over 1974-1976 (Fig. 4a). A weak warming is also seen over a relatively small coastal band between 50°W and 0°, with maximum values a bit lower than one degree in a few coastal regions. Those values on the continent are smaller than those observed at Halley station for the same time periods, suggesting either that the observed anomalies cannot be fully attributed to the polynya formation or that the simulations



underestimate the temperature changes over the continent due to the great Weddell Sea polynya formation, or a combination
290 of the two.

Precipitation in this simulation increases strongly over the polynya as well as over the continent between 50°W and 0° (Fig.
4b). However, precipitation tends to decrease between 0 and 50°E. Compared to observations, the signal appears thus more
contrasted and the increase is only clear over the continent westward of the Greenwich meridian, i.e. the region which is
downwind of the polynya for the dominant easterly winds. This is in agreement with the important role of the wind direction
295 in the location and amplitude of the temperature and precipitation signal related to polynya formation found in another model
(Weijer et al., 2017). The net change in snow accumulation in the simulation averaged over 1974-1976 and integrated over the
region 50°W -0 southward of 80°S is +13 Gt/y compared to the mean over the period 1958-2000 for the same region, a value
surprisingly close to the one in the reconstruction of Medley and Thomas (2019).

The $\delta^{18}\text{O}$ of precipitation is often related to temperature but the link can be weak and complex, in particular in coastal regions
300 of Antarctica where the impact of polynyas is expected to be the largest (e.g., Masson-Delmotte et al., 2008; Sime et al., 2008;
Holloway et al., 2016; Klein et al., 2019; Goursaud et al., 2019). This is even more problematic in the case of open polynya
formation where large changes in the seasonality of precipitation are expected. Nevertheless, the pattern of annual mean $\delta^{18}\text{O}$
of precipitation (Fig. 4c) associated to polynya formation is relatively similar to the one for the temperature, with for instance
high positive values over the polynya but only low positive ones over the continent except in a few regions close to the polynya.
305 The ice cores record the signal in the precipitation accumulated over one year at least (e.g., Stenni et al., 2017a) and the $\delta^{18}\text{O}$
of precipitation weighted by the amount of precipitation is a more adequate variable to compare to observed values. For this
diagnostic (Fig. 4d), the signal becomes even weaker over the continent, with only a few coastal regions where the anomaly
in annual mean $\delta^{18}\text{O}$ reaches 0.5 ‰.

Consequently, the analyses of observations and model results indicate that, although the maximum of the surface response to
310 polynya formation is expected over the ocean in winter, the polynya opening has likely induced a warming over the continent
in average over the period 1974-1976, as well as an increase in snow precipitation and a small modification of the $\delta^{18}\text{O}$ of
precipitation. However, the signal is not strong enough to detect without ambiguity the direct effects of the polynya compared
to other processes that can also lead to large interannual climate variations. Unfortunately, from polynya opening only during
3 years, we are unable to use any statistical test of significance that would give us a stronger conclusion.

315 In order to obtain complementary information on polynya dynamics and compare quantitatively the observed changes in the
1970s with the results of the SPEAR model, an index of open ocean convection and polynya activity is obtained in
SPEAR_AM2 and SPEAR_LO control simulations by calculating the annual mean mixed layer depth in the Eastern Weddell
sea between -50°W and 50°E southward of 60°S. Open convection occurs only in winter but the variability of the mixed layer
depth in the annual mean is controlled by the winter values. Therefore, using the annual mean avoids making an arbitrary
320 choice of which months to select for the average while convection can take place over a long period. Fig. 5 displays the



regression of temperature and precipitation with this index for the last 1000 years of the SPEAR_AM2 and SPEAR_LO simulations.

For the last 1000 years of the simulation, SPEAR_AM2 simulates recurring polynyas with centers around 20°E that induce a warming of up to 0.5°C per standard deviation of the index over the continent close to the coast. Precipitation over the continent
325 also increases in response to polynya formation, with a total increase of snow accumulation over the region 50°W-0, northward of 80°S of 17Gt/y per standard deviation of the index based on the mixed layer depth (30Gt/y per standard deviation for the region 50°W-50°E). This pattern is very similar to the one deduced both from the observations in the 1970s and the ECHAM5-wiso simulation.

In SPEAR_LO, the deep mixing and polynya formation in the Weddell Sea is concurrent with oceanic convection in the Ross
330 Sea (Zhang et al., 2020). Consequently, the warming and precipitation signal is more widespread over the continent. Close to the Greenwich meridian, the warming of the coastal regions is of the order of 0.5°C per standard deviation of the index as in SPEAR_AM2 simulation. The changes in snow accumulation over the region 50°W-0, northward of 80°S is 9 Gt/y per standard deviation of the index (41Gt/y per standard deviation for the region 50°W-50°E). Additionally, large warming and precipitation changes are observed in the simulation in the continental regions close to the Eastern Ross Sea and the Amundsen Sea.

335 **4 Reconstructing past polynya activity**

Standard methods applied to reconstructions covering the past millennium rely more or less directly on the correlation between the target (or predictand, here the polynya activity) and some predictors (for instance, selected ice core records) over the instrumental period in order to calibrate a statistical model (e.g., Mann et al., 2008; Jones et al., 2009; Christiansen and Ljungqvist, 2017; Stenni et al., 2017a). This statistical model is then applied over the full period were the predictors are
340 available to obtain a reconstruction of the target before the instrumental period. Here, this is not possible because the number of samples during the instrumental period is too small for any successful calibration. We thus have to propose a slightly different approach.

We first apply a simple reconstruction method centered on the average of the records that are the most likely influenced by the formation of big polynyas in the Weddell Sea. The selection of these records is based on the information provided in Sect. 3.
345 A large warming has been measured at Halley weather station in 1974-1976. However, the magnitude and the spatial extent of the temperature increase that can be directly attributed to polynya formation is ambiguous in observations and models. No direct long term temperature record is available as input for our reconstructions but high resolution temperature estimates before the instrumental period are often derived from the $\delta^{18}\text{O}$ measured in ice cores. The $\delta^{18}\text{O}$ signal over 1974-1976 in the simulation results is not very clear and relatively large values are restricted to a small continental region (Fig. 4d). Furthermore,
350 when analyzing the available $\delta^{18}\text{O}$ observations in the region close to the Weddell Sea, no well-defined pattern is identifiable (Fig. 2a). The closest records to Halley station (Berkner Island-South ice core, see Table 1) even display a decrease in $\delta^{18}\text{O}$ over the time period 1974-1976 while, with a simplistic interpretation, we would have expected a higher value associated with



the large warming observed in the region. Consequently, $\delta^{18}\text{O}$ records do not appear at this stage to be good candidates to reconstruct polynya activity with the simple methodology proposed here.

355 The impact of the polynyas on snow accumulation seems much more robust. The reconstructions based on ice cores, ECHAM5-wiso simulations for the 1970s and the control simulations with the SPEAR model all display an increase in the accumulation of similar magnitude between roughly 50°E and 0° in response to open ocean polynya formation. This higher accumulation has a clear and simple physical interpretation as stronger evaporation in the polynya region is expected to lead to more precipitation downwind. The signal over 1974-1976 from individual cores is not homogeneous (Fig. 3a) but this can
360 be related to the influence of local processes and post-depositional alterations in those records that may lead to relatively large differences even between nearby sites (Thomas et al., 2017; Laepple et al., 2019; Cavitte et al., 2020). Nevertheless, a large fraction of the cores in the region have values in 1974-1976 higher than the mean over 1958-2000 (Fig. 3a), which is of course consistent with the spatial reconstruction of Medley and Thomas (2019) based on those records.

Consequently, we propose to base our reconstruction on surface mass balance records only. We focus on records that are at
365 least 150 year-long to avoid too many changes in the number of records over the period of analysis (Table 1). The precise location of the western boundary of the region in which the sites are selected is not crucial because no record is available between Berkner Island (45.72°W) and the Antarctic Peninsula that is clearly out of the domain of direct influence of the great Weddell Sea polynya in our results. We will thus choose the limit at 50°W as in Sect. 3. For similar reasons, the southern boundary is set up 80°S . The choice for the eastern boundary requires a bit more attention as three records are located close to
370 the Greenwich Meridian in the data selected by Medley and Thomas (2019), but on its eastern side. We have therefore decided to keep the B40 (0.07°E), B33-DML17 (6.5°E) and Fimbulissen S100 (4.8°E) records, as it could be considered arbitrary to remove them while keeping nearby sites that are located just west of the Greenwich Meridian. If we move further eastward, the next site in the Medley and Thomas (2019) compilation is at 26.34°E (Derwael Ice Rise, Philippe et al., 2016), which is no longer in the region where all models and reconstructions agree on the impact of polynya formation on the surface mass
375 balance. Consequently, the final selection includes 6 sites (Table 1). As discussed in Sect. 2, all the time series are detrended over the period 1850-1992 and a 3-year running mean is applied prior to our analyses.

Since no direct calibration with instrumental observations of polynya activity is possible, we first standardize all the records by removing their mean and dividing by their standard deviation over the period 1941-1990. We then obtain the average of all
380 those standardized records to obtain a qualitative index of polynya occurrence. This simple average has a physical justification as the common signal associated with polynya formation should be positive in all the records as polynya opening leads to more precipitation in the whole region of interest. The index is then scaled to have a value of 1 in 1975, to have an easy comparison with the observed polynya in the years 1974-1976. The methodology could be considered as the equivalent of the classical composite plus scale approach but with a slightly different final step compared to previous studies that performed the scaling to fit with the observed variance of the reconstructed variable (e.g., Mann et al., 2008; Jones et al., 2009; Christiansen and
385 Ljungqvist, 2017; Stenni et al., 2017a).



The same records are used in the reconstructions with data assimilation. In theory, data assimilation should be able to handle observations outside of the region where the signal is the strongest. However, extracting the information on polynya activity potentially included in those records requires that the model simulates well the covariance between the regions where the polynya forms and the ones where those records are available. As it is difficult to evaluate the model performance on this aspect, we have preferred to focus on the six ice core records that are the most directly and strongly influenced by the polynya opening, like for the statistical method. As in Sect. 3, the index of polynya activity is computed from the annual mean mixed layer depth in the Eastern Weddell Sea between -50°W and 50°E . The index is scaled to have a value of 1 in 1975 and the average over the period 1941-1990 has been removed to be consistent with the simple statistical reconstruction.

Because of the small number of records and the difficulty to perform an independent validation, a formal investigation of the uncertainties of our reconstructions is out of the scope of this study. Nevertheless, the robustness of our results can be estimated by comparing the various indices proposed on Figs. 6 and 7. For the period 1250-1992, we provide one statistical reconstruction and two reconstructions with data assimilation using and SPEAR_AM2 and SPEAR_LO as priors, respectively. The two SPEAR simulations, which each display a polynya opening in a slightly different location in the Weddell Sea and an impact of these polynyas on snow accumulation over land characterized by a different pattern (Fig. 4), provide a rough range of the uncertainties associated to the simulation characteristics in data assimilation. The reconstructions are first based on the five (out of the six chosen) records available from 1250-1992 (Stat complete, DA SPEAR_AM2 complete and DA SPEAR_LO complete, Fig. 6a). Additionally, for each method, one reconstruction is performed for the years 1850-1992, using the additional record covering this period only (Stat all, DA SPEAR_AM2 all and DA SPEAR_LO all, Fig. 6b).

Over the last decades, all the times series show a clear maximum in 1975, corresponding well to the period 1974-1976 with the 3 year running mean applied. This implies that we are able to robustly reproduce the opening of the great Weddell Sea polynya. Smaller peaks are also observed in some reconstructions, for instance in 1983, while these years are not considered as particularly prone for the formation of smaller polynyas (Campbell et al., 2019). The index seems thus able to identify the known period with large open ocean polynyas but may have troubles to discriminate them clearly from years with high snow accumulation in the sector that may simply be caused by specific atmospheric conditions. The persistence of the polynyas over a few years helps to reduce the noise due to random atmospheric processes but this is likely not enough. It is reasonable to consider that large open ocean polynyas should systematically lead to a widespread anomaly in the surface mass balance in the continental region that is downwind from the polynya and thus a high value of the index. By contrast, a high snow accumulation is not necessarily caused by a polynya. In this framework, we can thus make the hypothesis that the index provides more 'false positive' for polynya events than events we completely miss.

Over the period 1850-1992, the maximum in nearly all the reconstructions is in 1882, with values often larger than in 1975. Relatively high values of the index are also found in 1934 in many reconstructions as well as some other peaks in individual reconstructions. Gordon (1982) made the hypothesis that a polynya occurred just before an oceanic cruise performed in 1962. The years before those observations are characterized by a prolonged period with a relatively high index in some reconstructions but no value above 0.75 in any of our reconstruction. Such values may correspond to the changes in the



420 accumulation due to polynyas smaller than the one observed in 1975, but this is impossible for us to determine if the explanation is valid from the available records.

For the pre-industrial period, high values of the index are found regularly in nearly every century. To be more quantitative, two threshold values for the index have been applied to detect polynya formation on Fig. 7. The value of 1 corresponds to events that have a similar imprint as the great Weddell polynya while events with a smaller impact over the continent can still
425 be detected with a value of 0.8. The years with an index higher than this value of 0.8 should still correspond to large events but the risk that a year with an index higher than 0.8 is not corresponding to an open ocean polynyas is higher (the ‘false positive’ mentioned above) than for a threshold of 1. Furthermore, the number of events seems less variable between the reconstruction methods using 0.8 than when using 1, at least during some periods.

The open ocean polynyas appear mainly as isolated events lasting a few years only, as observed in the 1970s. In addition to
430 the isolated events, more persistent sequences (although not continuous) are also reconstructed in particular over the periods 1350-1400 and 1600-1650 (Fig. 7). By contrast, no polynya is reconstructed during some other periods such as the years 1500-1550 in all the reconstructions and for both thresholds. This may be the signature of centennial-scale variability in polynya activity. Nevertheless, as we go back in time, the absence of event can simply be due to the dating uncertainties. A shift by a few years only between the records can lead to an event attributed to different years in the different time series and thus to a
435 muted value of the index when they are averaged. Low frequency variations of the surface mass balance in the sector, due to processes independent of polynya formation, could also modify the background state over which the polynya signal is imprinted. A higher mean accumulation would then lead to a higher chance to pass the threshold of 0.8 or 1 while a lower mean accumulation would imply that only the big polynyas would be detected. Finally, because of the detrending applied to the time series, we cannot compare the polynya activity over the past century with earlier periods.

440 5 Conclusions

Large and persistent open ocean polynyas have a major impact on the ocean surface at high latitudes, on ocean dynamics and on the deep ocean properties, as highlighted in many studies. Their imprint on the Antarctic continent has been much less investigated. Because of the small number of events, disentangling precisely the signal at the ice sheet surface coming from an open ocean polynya from other elements of the climate variability is impossible using the instrumental data only.
445 Nevertheless, instrumental data and surface mass balance reconstructions suggest a clear impact of the great Weddell Sea polynya in 1974-1976 on the continent, at least in the sector between roughly 50°W and 0°E. A comparison of the observed changes with the results of a model driven by observed sea surface temperature and sea ice concentration suggests an annual mean warming of less than one degree in coastal regions and an additional snow accumulation averaged over the sector of about 10 Gt/year during the polynya formation compared to average conditions.

450 Because of this impact of the open ocean polynyas on the Antarctic ice sheet, ice cores record can be used to reconstruct the occurrence of polynyas before the instrumental period. Surface mass balance records are the best candidates for an initial



reconstruction because of their availability in the region close to the Weddell Sea and polynya formation should be associated to, from robust physical arguments, an increase in snow accumulation in the sector downwind of the polynya. The signal is present in temperature as well but is weak for the isotopic composition of the snow, which is often considered as a proxy for temperature but whose interpretation is complex here in particular because of potential changes in the seasonality of precipitation due to open ocean polynya formation.

We have thus reconstructed an index of polynya activity based on the surface mass balance records in the sector 50°W and 5°E, using a simple average as well as data assimilation over the period 1250-1992. This reconstruction remains qualitative at present. The surface mass balance changes caused by polynya formation are not exceptional enough to distinguish the origin of a large value without ambiguity. Dating uncertainties in the records as well as low frequency variations in surface mass balance not related to polynya activity also complicate the detection of polynyas.

Additional information would be necessary to identify the years with a high value of the index but not corresponding to a polynya. Several proxies based on the chemical composition of Antarctic ice cores have been related to changes in sea ice concentrations (e.g., Abram et al., 2013; de Vernal et al., 2013; Thomas et al. 2019). The specific impact of a large open ocean polynya on those records is not well known but some of these variables have likely a signal related to polynya formation that is large enough to put additional constraints on the reconstructions and reduce our uncertainties. This provides thus a potential way to improve the estimates of changes in polynya occurrence over the past centuries.

Our reconstructions provide thus only a preliminary step whose goal is to stimulate more investigation on the subject. Our target is also limited to polynyas similar to the great Weddell polynya of the 1970s. This implies that we have not addressed the occurrence of smaller polynyas, that may be more frequent, or of open ocean polynyas that may have been present in other sectors of the Southern Ocean.

Despite those limitations, we are still able to reach some tentative conclusions about the frequency of polynya formation. First, the polynyas like the one observed in 1974-1976 are not frequent in the past millennium, occurring only a few times per century at most. Second, the sequences of polynya opening tend to last a few years only, with no clear periodicity. Some exceptions may have occurred with high surface mass balance values potentially associated with formation of polynyas during several decades. Nevertheless, as we go back in time, the uncertainties on the potential processes controlling the precipitation are larger, as are the dating uncertainties. Third, on a more technical point of view, the observed changes associated to polynya formation are similar to the ones given by global climate models that display realistic open ocean polynyas in the Weddell Sea, indicating that those models can be used for data assimilation. This technique is thus very promising for future reconstructions of polynya activity.

Data availability. Instrumental observations can be obtained on the READER site (<https://legacy.bas.ac.uk/met/READER/>, last access: 9 April 2020). The reconstruction of Antarctic surface air temperatures based on instrumental data is available at http://polarmet.osu.edu/datasets/Antarctic_recon/ (last access: 4 July 2018, Nicolas and Bromwich, 2014b). $\delta^{18}\text{O}$ time series are available at the NOAA World Data Center for Paleoclimatology (<https://www.ncdc.noaa.gov/paleo-search/study/22589>,



last access: 18 March 2018, Stenni et al., 2017b). The surface mass balance time series comes from <https://data.bas.ac.uk/full-record.php?id=GB/NERC/BAS/PDC/00940> and the reconstruction of Medley and Thomas (2019) is available at <https://earth.gsfc.nasa.gov/cryo/data/antarctic-accumulation-reconstructions>. The results of the ECHAM5-wiso simulation covering the 1871–2011 period can be downloaded from <https://doi.org/10.5281/zenodo.1249604> (Steiger, 2018). RACMO2
490 data are available by request to Jan Lenaerts (jan.lenaerts@Colorado.EDU). The SPEAR-LO and SPEAR-AM2 results are available by request to Liping Zhang (liping.zhang@noaa.gov). The reconstruction of polynya activity will be posted on a public repository when the final version of the manuscript and thus of the reconstruction will be accepted for publication.

Competing interests. The authors declare that there is no conflict of interest.

495

Acknowledgements. This work was supported by the Belgian Research Action through Interdisciplinary Networks (BRAINbe) from Belgian Science Policy Office in the framework of the project “East Antarctic surface mass balance in the Anthropocene: observations and multiscale modelling (Mass2Ant)” (contract no. BR/165/A2/Mass2Ant). Hugues Goosse is the research director within the F.R.S.-FNRS. Quentin Dalaiden is a research fellow with the Fonds pour la formation á la
500 Recherche dans l’Industrie et dans l’Agriculture (FRIA-Belgium). L. Zhang is supported through UCAR under block funding from NOAA/GFDL. We would like to thank all the scientists that collected and share their ice core records as well Nathan Steiger for sharing the output of the ECHAM5-wiso simulation, Jan Lenaerts for sharing the output of the RACMO simulation and Rachael Rhodes, Jean-Louis Tison and François Fripiat for stimulating discussions on polynya reconstructions.

References

- 505 Abram, N.J., Wolff, E.W., and Curran, M.A.J.: A review of sea ice proxy information from polar ice cores, *Quat. Sci. Rev.*, 79, 168–183, <https://doi.org/10.1016/j.quascirev.2013.01.011>, 2013.
- Adcroft, A., Anderson, W., Balaji, V., Blanton, C., Bushuk, M., Dufour, C.O., Dunne, J.P., Griffies, S.M., Hallberg, R., J. Harrison, M.J., Held, I.M., Jansen, M.F., John, J.G., Krasting, J.P., Langenhorst, A.R., Legg, S., Liang, Z., McHugh, C., Radhakrishnan, A., Reichl, B.G., Rosati, T., Samuels, B.L., Shao, A., Stouffer, R., Winton, M., Wittenberg, A.T., Xiang, B.,
510 Zadeh, N., and Zhang, R.: The GFDL global ocean and sea ice model OM4.0: Model description and simulation features, *J. Adv. Model. Earth Syst.*, 11, doi:10.1029/2019MS001726, 2019.
- Anderson, J. L., and Coauthors: The new GFDL global atmosphere and land model AM2–LM2: Evaluation with prescribed SST simulations, *J. Climate*, 17, 4641–4673, <https://doi.org/10.1175/JCLI-3223.1>, 2004.
- Badgeley, J.A., Steig, E. J., Hakim, G. J., and Fudge, T. J.: Greenland temperature and precipitation over the last 20,000 years
515 using data assimilation, Submitted to *Clim. Past*, <https://doi.org/10.5194/cp-2019-164>, 2020.



- Behrens, E., Rickard, G., Morgenstern, O., Martin, T., Osprey, A., and Joshi, M.: Southern Ocean deep convection in global climate models: A driver for variability of subpolar gyres and Drake Passage transport on decadal timescales, *J. Geophys. Res. Oceans*, 121, 3905–3925, <https://doi.org/10.1002/2015JC011286>, 2016.
- 520 Campbell, E.C., Wilson, E. A., Moore, G. W. K., Riser, S. C., Brayton, C. E., Mazloff, M. R., and Talley, L. D.: Antarctic offshore polynyas linked to Southern Hemisphere climate anomalies, *Nature*, 570, 319–325, doi: 10.1038/s41586-019-1294-0, 2019.
- Carsey F. D.: Microwave observation of the Weddell Polynya, *Mon. Weath. Rev.*, 108, 2032–2044, [https://doi.org/10.1175/1520-0493\(1980\)108<2032:MOOTWP>2.0.CO;2](https://doi.org/10.1175/1520-0493(1980)108<2032:MOOTWP>2.0.CO;2), 1980.
- 525 Cavitte, M.G.P., Dalaiden, Q., and Goosse, H.: Reconciling the link between surface temperature–surface mass balance between models and ice cores, Submitted to *The Cryosphere*, <https://www.the-cryosphere-discuss.net/tc-2020-36/>, 2020.
- Cheon, W. G., Lee, S.-K., Gordon, A. L., Liu, Y., Cho, C.-B., and Park, J. J.: Replicating the 1970s’ Weddell Polynya using a coupled ocean-sea ice model with reanalysis surface flux fields, *Geophys. Res. Lett.*, 42, 5411–5418, <https://doi.org/10.1002/2015GL064364>, 2015.
- Christiansen, B., and Ljungqvist F. C.: Challenges and perspectives for large-scale temperature reconstructions of the past two
530 millennia, *Rev. Geophys.*, 55, doi:10.1002/2016RG000521, 2017.
- Comiso, J.C. and Gordon, A.L.: Recurring polynyas over the Cosmonaut Sea and the Maud Rise, *J. Geophys. Res.* 92, 2819–2833, <https://doi.org/10.1029/JC092iC03p02819>, 1987.
- Comiso, J.C. and Gordon, A.L.: Cosmonaut polynya in the Southern Ocean: structure and variability, *J. Geophys. Res.* 101, 18297–18313, <https://doi.org/10.1029/96JC01500>, 1996.
- 535 Dalaiden, Q., Goosse, H., Klein, F., Lenaerts, J., Holloway, M., Sime, L., and Thomas, L.: How useful is snow accumulation in reconstructing surface air temperature in Antarctica? A study combining ice core records and climate models, *The Cryosphere*, 14, 1187–1207. <https://doi.org/10.5194/tc-2019-111>, 2020.
- de Lavergne C., Palter, J.B., Galbraith, E.D., Bernardello, R., and Marinova, I.: Cessation of deep convection in the open Southern Ocean under anthropogenic climate change, *Nat. Clim. Change*, 4, 278–282, <https://doi.org/10.1038/nclimate2132>,
540 2014.
- de Vernal A., Gersonde, R., Goosse, H., Seidenkrantz, M.-S., and Wolff, E. W.: Sea ice in the paleoclimate system: the challenge of reconstructing sea ice from proxies- An introduction, *Quat. Science Rev.*, 79, 1–8. doi: 10.1016/j.quascirev.2013.08.009, 2013.
- 545 Delworth, T. L., Cooke, W.F., Adcroft, A., Bushuk, M., Chen, J.-H., Dunne, K.A., Ginoux, P., Gudgel, R., Hallberg, R.W., Harris, L., J. Harrison, M.J., Johnson, N., Kapnick, S.B., Lin, S.J., Lu, F., Malyshev, S., Milly, P. C., Murakami, H., Naik, V., Pascale, S. Paynter, D., Rosati, A., Schwarzkopf, M.D., Shevliakova, E., Underwood, S., Wittenberg, A.T., Xiang, B., Yang, X. Zeng, F. Zhang, H. Zhang, and L., Zhao, M.: SPEAR-the next generation GFDL modeling system for seasonal to



- multidecadal prediction and projection, *J. Advan. Mod. Earth Sys*, 12, e2019MS0018952020, <https://doi.org/10.1029/2019MS001895>, 2020.
- 550 Dubinkina, S., and Goosse, H.: An assessment of particle filtering methods and nudging for climate state reconstructions, *Clim. Past*, 9, 1141–1152, <https://doi.org/10.5194/cp-9-1141-2013>, 2013.
- Dufour, C.O., Morrison, A.K., Griffies, S.M., Frenger, I., Zanowski, H., and Winton, M.: Preconditioning of the Weddell Sea polynya by the ocean mesoscale and dense water overflows, *J. Clim.*, 30, 7719–7737, <https://doi.org/10.1175/JCLI-D-16-0586.1>, 2017.
- 555 Francis, D., Eayrs, C., Cuesta, J., and Holland, D.: Polar cyclones at the origin of the reoccurrence of the Maud Rise Polynya in austral winter 2017, *J. Geophys. Res. Atmos.*, 124, 5251–5267, <https://doi.org/10.1029/2019JD030618>, 2019.
- Foster T.D., and Carmack, E.C.: Frontal zone mixing and Antarctic Bottom Water formation in the southern Weddell Sea. *Deep Sea Res. Oceanogr. Abstr.* 23 (4), 301–317, [https://doi.org/10.1016/0011-7471\(76\)90872-X](https://doi.org/10.1016/0011-7471(76)90872-X), 1976.
- Franke, J., Brönnimann, S., Bhend, J., and Brugnara, Y.: A monthly global paleo-reanalysis of the atmosphere from 1600 to
560 2005 for studying past climatic variations, *Scientific Data* 4, 2017, Article number 170076, doi: 10.1038/sdata.2017.76, 2017.
- Goosse, H. and Fichefet, T.: Open-ocean convection and polynya formation in a large-scale ice-ocean model, *Tellus*, 53A, 94–111, DOI: 10.1034/j.1600-0870.2001.01061.x, 2001.
- Goosse, H., Crespin, E., Dubinkina, S., Loutre, M.F., Mann, M. E., Renssen, H., Sallaz-Damaz, Y., and Shindell, D.: The role of forcing and internal dynamics in explaining the “Medieval Climate Anomaly”, *Clim. Dyn.*, 39, 2847–2866, doi: 10.1007/s00382-012-1297-0, 2012.
- 565 Goosse, H., Kay, J. E., Armour, K., Bodas-Salcedo, A., Chepfer, H., Docquier, D., Jonko, A., Kushner, P. J., Lecomte, O., Massonnet, F., Park, H.-S., Pithan, F., Svensson, G., and Vancoppenolle, M.: Quantifying climate feedbacks in polar regions, *Nat. Com.*, 9, 1919, DOI: 10.1038/s41467-018-04173-0, <https://rdcu.be/OjXE>, 2018.
- Gordon, A. L.: Deep Antarctic convection west of Maud Rise. *J. Phys. Oceanogr.*, 8, 600–612, [https://doi.org/10.1175/1520-0485\(1978\)008<0600:DACWOM>2.0.CO;2](https://doi.org/10.1175/1520-0485(1978)008<0600:DACWOM>2.0.CO;2) 1978.
- 570 Gordon, A.L.: Weddell Deep Water variability, *J.Mar. Res.*, 40 (suppl.), 199–217, 1982.
- Gordon, A.L. and Huber, B.A.: Southern Ocean winter mixed layer, *J. Geophys. Res.* 95(C7), 11655–11672, <https://doi.org/10.1029/JC095iC07p11655>, 1990
- Gordon, A.L., Visbeck, M., and Comiso, J.C.: A possible link between the Weddell Polynya and the Southern Annular Mode, *J. Clim.*, 20, 2558–2571, <https://doi.org/10.1175/JCLI4046.1>, 2007.
- 575 Gorodetskaya, I. V., Tsukernik, M., Claes, K., Ralph, M. F., Neff, W. D., and van Lipzig, N. P. M.: The role of atmospheric rivers in anomalous snow accumulation in East Antarctica, *Geophys. Res. Lett.*, 41, 6199–6206. <https://doi.org/10.1002/2014GL060881>, 2014.



- Goursaud, S., Masson-Delmotte, V., Favier, V., Preunkert, S., Legrand, M., Minster, B., and Werner M.: Challenges associated with the climatic interpretation of water stable isotope records from a highly resolved firn core from Adélie Land, coastal Antarctica, *The Cryosphere*, 13, 1297–1324, <https://doi.org/10.5194/tc-13-1297-2019>, 2019.
- Graf, W., Oerter H., Reinwarth, O., and Stichler, W.: Stable-isotope records from Dronning Maud Land, Antarctica. *Ann. Glaciol.* 35, 195-201, <https://doi.org/10.3189/172756402781816492>, 2002.
- Hakim, G.J., Emile-Geay, J., Steig, E.J., Noone, D., Anderson, D.M., Tardif, R., Steiger, N., and Perkins, W.A.: The last millennium climate reanalysis project: Framework and first results, *J. Geophys. Research* 121, 6745-6764, <https://doi.org/10.1002/2016JD024751>, 2016.
- Heuzé, C., Heywood, K. J., Stevens, D. P., and Ridley, J. K.: Southern Ocean bottom water characteristics in CMIP5 models, *Geophys. Res. Lett.*, 40, 1409–1414, doi:10.1002/grl.50287, 2013.
- Heuzé C., Heywood, K. J., Stevens, D. P., Ridley, J. K.: Changes in global ocean bottom properties and volume transports in CMIP5 models under climate change scenarios, *J. Clim.*, 28, 2917–2944, <https://doi.org/10.1175/JCLI-D-14-00381.1>, 2015.
- Holland D.M.: Explaining the Weddell Polynya – a large ocean eddy shed at Maud Rise, *Science*, 292 1697-1700, doi: 10.1126/science.1059322, 2001.
- Holloway, M.D., L. C. Sime, J. S. Singarayer, J. C. Tindall, P. Bunch, and Valdes, P. J.: Antarctic last interglacial isotope peak in response to sea ice retreat not ice-sheet collapse, *Nat. Com.* 7, Article number: 12293, <https://doi.org/10.1038/ncomms12293>, 2016.
- Janjić, T., Bormann, N., Bocquet, M., Carton, J. A., Cohn, S. E., Dance, S. L., Losa, S. N., Nichols, N. K., Potthast, R., Waller, J. A. and Weston, P.: On the representation error in data assimilation, *Advances in Data Assimilation Methods*, *Quat. J. R. Met. Soc.*, 144 (713), Part B 1257-1278, <https://doi.org/10.1002/qj.3130>, 2018.
- Jena, B., Ravichandran, M., and Turner, J.: Recent reoccurrence of large open-ocean polynya on the Maud Rise seamount, *Geophys. Res. Lett.*, 46, 4320–4329, <https://doi.org/10.1029/2018GL081482>, 2019.
- Johnson, G. C.: Quantifying Antarctic Bottom Water and North Atlantic Deep Water volumes, *J. Geophys. Res.*, 113, C05027, doi:10.1029/2007JC004477, 2008.
- Jones, P.D., Briffa, K.R., Osborn, T.J., Lough, J. M., van Ommen, T., Vinther, B.M., Luterbacher, J., Zwiers, F.W., Wahl, E., Schmidt, G., Ammann, C., Mann, M.E., Wanner, H., Buckley, B.M., Cobb, K., Esper, J., Gooose, H., Graham, N., Jansen, E., Kiefer, T., Kull, C., Mosley-Thompson, E., Overpeck, J.T., Schulz, M., Tudhope, S., Villalba, R. and Wolff, E.: High-resolution paleoclimatology of the last millennium: a review of the current status and future prospects, *The Holocene*, 19, 3-49, <https://doi.org/10.1177/0959683608098952> 2009.
- Jüling, A., Viebahn, J.-P., Drijfhout, S.S., and Dijkstra, H.A.: Energetics of the Southern Ocean Mode, *J. Geophys. Res. Oceans*, 123, 9283–9304, <https://doi.org/10.1029/2018JC014191>, 2018.



- 610 Kaufman, Z.S., Feldl, N., Weijer, W., and Veneziani, M.: Causal interactions between Southern Ocean polynyas and high-latitude atmosphere–ocean variability, *J.Clim.*, 33, 4891–4905, <https://doi.org/10.1175/JCLI-D-19-0525.1>, 2020.
- Kaczmarska, M., Isaksson, E., Karlöf, K., Winther, J.-G., Kohler, J., Godtliessen, F., Ringstad Olsen, L., Hofstede, C. M., van den Broeke, M. R., Van DeWal, R. S.W., and Gundestrup, N.: Accumulation variability derived from an ice core from coastal Dronning Maud Land, Antarctica, *Annals of Glaciology*, 39, 339–345, DOI: <https://doi.org/10.3189/172756404781814186>,
615 2004.
- Kerr, R., Dotto, T.S., Mata, M. M., and Hellmer, H. H.: Three decades of deep water mass investigation in the Weddell Sea (1984–2014): Temporal variability and changes, *Deep Sea Res. Part II*, 149, 70–83, <https://doi.org/10.1016/j.dsr2.2017.12.002>, 2018.
- Klein, F., Abram, N. J., Curran, M. A. J., Goose, H., Goursaud, S., Masson-Delmotte, V., Moy, A., Neukom, R., Orsi, A.,
620 Sjolte, J., Steiger, N., Stenni, B. and Werner, M.: Assessing the robustness of Antarctic temperature reconstructions over the past two millennia using pseudoproxy and data assimilation experiments, *Clim. Past* 15, 661–684, <https://doi.org/10.5194/cp-15-661-2019>, 2019.
- Kurtakoti P., Veneziani, M., Stössel, A., and Weijer, W.: Preconditioning and formation of Maud Rise polynyas in a high-resolution Earth System Model, *J. Clim.*, 31, 9659–9678, <https://doi.org/10.1175/JCLI-D-18-0392.1>, 2018.
- 625 Laepple, T., Münch, T., Casado, M., Hoerhold, M., Landais, A., and Kipfstuhl, S.: On the similarity and apparent cycles of isotopic variations in East Antarctic snow pits, *The Cryosphere*, 12, 169–187, <https://doi.org/10.5194/tc-12-169-2018>, 2018.
- Laluraj, C.M., Thamban, M., Naik, S.S., Redkar, B.L., Chaturvedi, A., and Ravindra, R.: Nitrate records of a shallow ice core from East Antarctica: atmospheric processes, preservation and climatic implications, *The Holocene*, 21, 351–356, DOI: 10.1177/0959683610374886, 2011.
- 630 Latif, M., Martin, T., and Park, W.: Southern Ocean sector centennial climate variability and recent decadal trends, *J. Clim.*, 26, 7767–7782, <https://doi.org/10.1175/JCLI-D-12-00281.1>, 2013.
- Le Bars, D., Viebahn, J.P., and Dijkstra, H.A.: A Southern Ocean mode of multidecadal variability, *Geophys. Res. Lett.*, 43, 2102–2110, <https://doi.org/10.1002/2016GL068177>, 2016.
- Lenaerts, J. T. M., Medley, B., van den Broeke, M. R., and Wouters, B.: Observing and modeling ice sheet surface mass
635 balance, *Reviews of Geophysics*, 57, <https://doi.org/10.1029/2018RG000622>, 2019.
- Lyman, J.M. and Johnson, G. C.: Estimating global ocean heat content changes in the upper 1800 m since 1950 and the influence of climatology choice, *J. Clim.*, 27, 1945–1957, <https://doi.org/10.1175/JCLI-D-12-00752.1> 2014.
- Manabe, S., Stouffer, R.J., Spelman, M.J., and Bryan, K.: Transient response of coupled ocean-atmosphere model to gradual changes of atmospheric CO₂, *J. Climate*, 4, 785–818, [https://doi.org/10.1175/1520-0442\(1991\)004<0785:TROACO>2.0.CO;2](https://doi.org/10.1175/1520-0442(1991)004<0785:TROACO>2.0.CO;2),
640 1991.



- Mann, M. E., Zhang, Z., Hughes, M.K., Bradley, R. S., Miller, S. K., Rutherford S., and Ni, F.: Proxy-based reconstructions of hemispheric and global surface temperature variations over the past two millennia, *Proc. Natl Acad. Sci. USA*, 105, 1325213257, <https://doi.org/10.1073/pnas.0805721105>, 2008.
- Mantyla, A.W. and Reid, J.L.: Abyssal characteristics of the World Ocean waters, *Deep Sea Res. Part A*, 30, 805-833, [https://doi.org/10.1016/0198-0149\(83\)90002-X](https://doi.org/10.1016/0198-0149(83)90002-X), 1983
- 645 Marshall, G.J.: Trends in the Southern Annular Mode from observations and reanalyses, *J. Clim.*, 16, 4134-4143, [https://doi.org/10.1175/1520-0442\(2003\)016<4134:TITSAM>2.0.CO;2](https://doi.org/10.1175/1520-0442(2003)016<4134:TITSAM>2.0.CO;2), 2003.
- Martin T., Park, W., and Latif, M.: Multi-centennial variability controlled by Southern Ocean convection in the Kiel Climate Model, *Clim. Dyn.*, 40, 2005–2022, <https://doi.org/10.1007/s00382-012-1586-7>, 2013.
- 650 Martinson D. G., Killworth, P.D., and Gordon, A.L.: A convective model for the Weddell Polynya, *J. Phys. Oceanogr.*, 11, 466-488, [https://doi.org/10.1175/1520-0485\(1981\)011<0466:ACMFTW>2.0.CO;2](https://doi.org/10.1175/1520-0485(1981)011<0466:ACMFTW>2.0.CO;2), 1981.
- Martinson, D.G.: Evolution of the Southern Ocean winter mixed layer and sea ice: open ocean deepwater formation and ventilation, *J. Geophys. Res.*, 95(C7), 11641-11654, <https://doi.org/10.1029/JC095iC07p11641>, 1990.
- Masson-Delmotte, V., Hou, S., Ekaykin, A., Jouzel, J., Aristarain, A., Bernardo, R., Bromwich, D., Cattani, O., Delmotte, M., Falourd, S., Frezzotti, M., Gallée, H., Genoni, L., Isaksson, E., Landais, A., Helsen, M., Hoffmann, G., Lopez, J., Morgan, V., Motoyama, H., Noone, D., Oerter, H., Petit, J., Royer, A., Uemera, R., Schmidt, G., Schlosser, E., Simões, J., Steig, E., Stenni, B., Stievenard, M., van den Broeke, M., van de Wal, R., van de Berg, W., Vimeux, F., White, J.: A review of Antarctic surface snow isotopic composition: Observations, atmospheric circulation, and isotopic modeling, *J. Clim.*, 21, 3359–3387, <https://doi.org/10.1175/2007JCLI2139.1>, 2008.
- 655 Medley, B. and Thomas, E. R.: Increased snowfall over the Antarctic Ice Sheet mitigated twentieth-century sea-level rise, *Nat. Clim. Change*, 9(1), 34–39, <https://doi.org/10.1038/s41558-018-0356-x>, 2019.
- Medley, B., McConnell, J. R., Neumann, T. A., Reijmer, C. H., Chellman, N., Sigl, M., and Kipfstuhl, S.: Temperature and snowfall in western Queen Maud Land increasing faster than climate model projections. *Geophys. Res. Lett.*, 45, 1472–1480. <https://doi.org/10.1002/2017GL075992>, 2018.
- 660 Moore, G. W. K., Alverson, K., and Renfrew, I. A.: A reconstruction of the air–sea interaction associated with the Weddell Polynya, *J. Phys. Oceanogr.*, 32, 1685–1698, doi:10.1175/1520-0485(2002)032,1685:AROTAS.2.0.CO;2, 2002.
- Morales Maqueda M. A., Willmott, A. J., and Biggs, N. R. T.: Polynya dynamics: A review of observations and modeling, *Rev. Geophys.*, 42, RG1004, doi:10.1029/2002RG000116, 2004.
- Mulvaney, R., Oerter, H., Peel, D. A., Graf, W., Arrowsmith, C., Pasteur, E. C., Knight, B., Littot, G. C., and Miners, W. D.: 1000 year ice-core records from Berkner Island, Antarctica, *Ann. Glaciol.*, 35, 45–51, <https://doi.org/10.3189/172756402781817176>, 2002.
- 670



- Nicolas J. P. and Bromwich, D.H.: New reconstruction of Antarctic near-surface temperatures: Multidecadal trends and reliability of global reanalyses, *J. Clim.*, 27, 8070–8093, <https://doi.org/10.1175/JCLI-D-13-00733.1> 2014a.
- Nicolas, J. P. and Bromwich, D. H.: Reconstruction of Antarctic near-surface temperatures (1958–2012), Data set, Polar
675 Meteorology Group, available at: http://polarmet.osu.edu/datasets/Antarctic_recon/ (last access: 4 July 2018), 2014b.
- Nishio, F., Furukawa, T., Hashida, G., Igarashi, M., Kameda, T., Kohno, M., Motoyama, H., Naoki, K., Satow, K., Suzuki, K., Morimasa, T., Toyama, Y., Yamada, T., and Watanabe, O.: Annual-layer determinations and 167 year records of past climate of H72 ice core in east Dronning Maud Land, Antarctica, *Ann. Glaciol.*, 35, 471–479, <https://doi.org/10.3189/172756402781817086>, 2002.
- 680 Oerter, H., Wilhelms, F., Jung-Rothenhäusler, F., Göktas, F., Miller, H., Graf, W., and Sommer, S.: Accumulation rates in Dronning Maud Land, Antarctica, as revealed by dielectric-profiling measurements of shallow firn cores, *Ann. Glaciol.*, 30, 27–34, <https://doi.org/10.3189/172756400781820705>, 2000.
- Philippe, M., Tison, J.-L., Fjøsne, K., Hubbard, B., Kjær, H. A., Lenaerts, J. T. M., Drews, R., Sheldon, S. G., De Bondt, K., Claeys, P., and Pattyn, F.: Ice core evidence for a 20th century increase in surface mass balance in coastal Dronning Maud
685 Land, East Antarctica, *The Cryosphere*, 10, 2501–2516, <https://doi.org/10.5194/tc-10-2501-2016>, 2016.
- Purkey, S.G., Smethie Jr., W. M., Gebbie, G., Gordon, A. L., Sonnerup, R. E., Warner, M. J., and Bullister, J. L.: A synoptic view of the ventilation and circulation of Antarctic Bottom Water from chlorofluorocarbons and natural tracers, *Annu. Rev. Mar. Sci.*, 10:503–27, DOI: 10.1146/annurev-marine-121916-063414, 2018.
- Rayner, N.A., Parker, D.E., Horton, E.B., Folland, C.K., Alexander, L.V., Rowell, D.P., Kent, E.C., and Kaplan, A.: Global
690 analyses of sea surface temperature, sea ice, and night marine air temperature since the late nineteenth century, *J. Geophys. Res. Atmos.* 108, 4407, <https://doi.org/10.1029/2002JD002670>, 2003.
- Resplandy, L., Keeling, R. F., Eddebbar, Y., Brooks, M. K., Wang, R., Bopp, L., Long, M. C., Dunne, J. P., Koeve, W., and Oschlies, A.: Quantification of ocean heat uptake from changes in atmospheric O₂ and CO₂ composition, *Nature*, 563, 105–108, <https://doi.org/10.1038/s41586-018-0651-8>, 2018.
- 695 Robertson, R., Visbeck, M., Gordon, A. L., and Fahrback, E.: Long-term temperature trends in the deep waters of the Weddell Sea, *Deep-Sea Research II*, 49, 4791–4806, [https://doi.org/10.1016/S0967-0645\(02\)00159-5](https://doi.org/10.1016/S0967-0645(02)00159-5), 2002.
- Sallée, J.-B., Shuckburgh, E., Bruneau, N., Meijers, A. J. S., Bracegirdle, T. J., Wang, Z., and Roy, T.: Assessment of Southern Ocean water mass circulation and characteristics in CMIP5 models: Historical bias and forcing response, *J. Geophys. Res. Oceans*, 118, 1830–1844, doi:10.1002/jgrc.20135, 2013.
- 700 Sime, L.C., Tindall, J.C., Wolff, E.W., Connolley, W.M., and Valdes, P.: Antarctic isotopic thermometer during a CO₂ forced warming event, *J. Geophys. Res.* 113, D24119, doi: 10.1029/2008JD010395, 2008.



- Sommer, S., Appenzeller, C., Rothlisberger, R., Hutterli, M. A., Stauffer, B., Wagenbach, D., Oerter, H., Wilhelms, F., Miller, H., and Mulvaney, R.: Glacio-chemical study spanning the past 2 kyr on three ice cores from Dronning Maud Land, Antarctica 1. Annually resolved accumulation rates, *J. Geophys. Res.*, 105, 29411–29421, <https://doi.org/10.1029/2000JD900449>, 2000.
- 705 Steig, E. J., Ding, Q., White, J. W. C., Küttel, M., Rupper, S. B., Neumann, T. A., Neff, P. D., Gallant, A. J. E., Mayewski, P. A., Taylor, K. C., Hoffmann, G., Dixon, D. A., Schoenemann, S. W., Markle, B. R., Fudge, T. J., Schneider, D. P., Schauer, A. J., Teel, R. P., Vaughn, B. H., Burgener, L., Williams, J., and Korotkikh E.: Recent climate and icesheet changes in West Antarctica compared with the past 2,000 years, *Nat. Geosci.*, 6, 372–375, doi:10.1038/ngeo1778, 2013.
- Steiger, N. J., Steig, E. J., Dee, S. G., Roe, G. H., and Hakim, G. J.: Climate reconstruction using data assimilation of water isotope ratios from ice cores, *J. Geophys. Res.-Atmos.*, 122, 1545–1568, <https://doi.org/10.1002/2016JD026011>, 2017.
- 710 Steiger, N. J.: Historical climate model output of ECHAM5- wiso from 1871–2011 at T106 resolution, Data set, Zenodo, <https://doi.org/10.5281/zenodo.1249604>, 2018.
- Steiger, N.J., Smerdon, J.E., Cook, E.R., Cook, B.I.: A reconstruction of global hydroclimate and dynamical variables over the Common Era, *Scientific Data*, 5, 22, Article number 180086b, <https://doi.org/10.1038/sdata.2018.86>, 2018.
- 715 Stenni, B., Curran, M. A. J., Abram, N. J., Orsi, A., Goursaud, S., Masson-Delmotte, V., Neukom, R., Goosse, H., Divine, D., van Ommen, T., Steig, E. J., Dixon, D. A., Thomas, E. R., Bertler, N. A. N., Isaksson, E., Ekaykin, A., Werner, M., and Frezzotti, M.: Antarctic climate variability on regional and continental scales over the last 2000 years, *Clim. Past*, 13, 1609–1634, <https://doi.org/10.5194/cp-13-1609-2017>, 2017a.
- Stenni, B., Curran, M. A. J., Abram, N. J., Orsi, A. J., Goursaud, S., Masson-Delmotte, V., Neukom, R., Goosse, H., Divine, D. V., van Ommen, T. D., Steig, E. J., Dixon, D. A., Thomas, E. R., Bertler, N. A. N., Isaksson, E., Ekaykin, A. A., Werner, M., and Frezzotti, M.: PAGES Antarctica2k Temperature Reconstructions, Data set, NOAA, available at: <https://www.ncdc.noaa.gov/paleo-search/study/22589> (last access: 18 March 2018), 2017b.
- 720 Stössel, A. and Kim, S.-J.: Decadal deep-water variability in the subtropical Atlantic and convection in the Weddell Sea, *J. Geophys. Res.*, 106, 22 425–22 440, <https://doi.org/10.1029/2000JC000335>, 2001.
- 725 Stössel, A., Notz, D., Haumann, F. A., Haak, H., Jungclaus, J., Mikolajewicz, U.: Controlling high-latitude Southern Ocean convection in climate models, *Ocean Modell.*, 86, 58–75, <https://doi.org/10.1016/j.ocemod.2014.11.008>, 2015.
- Swart, S., Johnson, K., Mazloff, M. R., Meijers, A., Meredith, M. P., Newman, L., and Sallée, J.-B.: Return of the Maud Rise polynya: climate litmus or sea ice anomaly? [in "State of the Climate in 2017"]. *Bull. Am. Meteorol. Soc.*, 99, S188–S189, doi: 10.1175/2018BAMSStateoftheClimate.1, 2018.
- 730 Timmermann, R., Lemke, P., and Kottmeier, C.: Formation and maintenance of a polynya in the Weddell Sea, *J. Phys. Oceanogr.*, 29, 1251–1264, DOI: 10.1175/1520-0485(1999)029<1251:FAMOAP>2.0.CO;2 1999.
- Thomas, E. R., van Wesse, J. M., Roberts, J., Isaksson, E., Schlosser, E., Fudge, T. J., Vallelonga, P., Medley, B., Lenaerts, J., Bertler, N., van den Broeke, M. R., Dixon, D. A., Frezzotti, M., Stenni, B., Curran, M., and Ekaykin, A. A.: Regional



- Antarctic snow accumulation over the past 1000 years, *Clim. Past*, 13, 1491–1513, <https://doi.org/10.5194/cp-13-1491-2017>,
735 2017.
- Thomas, E.R., Allen, C. S., Etourneau, J., King, A. C. F., Severi, M., Winton, V. H. L., Mueller, J., Crosta, X., and Peck, V.L.: Antarctic sea ice proxies from marine and ice core archives suitable for reconstructing sea ice over the past 2000 Years, *Geosciences*, 9, 506; doi:10.3390/geosciences9120506, 2019.
- Turner, J., Colwell, S. R., Marshall, G. J., Lachlan-Cope, T. A., Carleton, A. M., Jones, P. D., Lagun, V., Reid, P. A., and
740 Iagovkina, S.: The SCAR READER project: Toward a high-quality database of mean Antarctic meteorological observations, *J. Clim.*, 17, 2890–2898, [https://doi.org/10.1175/1520-0442\(2004\)017<2890:TSRPTA>2.0.CO;2](https://doi.org/10.1175/1520-0442(2004)017<2890:TSRPTA>2.0.CO;2), 2004.
- Turner, J., Phillips, T., Thamban, M., Rahaman, W., Marshall, G. J., Wille, J. D., Vincent, V., Winton, V. Holly, L., Thomas, E., Wang, Z., van den Broeke, M., Hosking, J. S., and Lachlan-Cope, T.: The dominant role of extreme precipitation events in Antarctic snowfall variability, *Geophys. Res. Lett.*, 46, 3502–3511, <https://doi.org/10.1029/2018GL081517>, 2019.
- 745 van Wessem, J. M., van de Berg, W. J., Noël, B. P. Y., van Meijgaard, E., Amory, C., Birnbaum, G., Jakobs, C. L., Krüger, K., Lenaerts, J. T. M., Lhermitte, S., Ligtenberg, S. R. M., Medley, B., Reijmer, C. H., van Tricht, K., Trusel, L. D., van Uft, L. H., Wouters, B., Wuite, J., and van den Broeke, M. R.: Modelling the climate and surface mass balance of polar ice sheets using RACMO2 – Part 2: Antarctica (1979–2016), *The Cryosphere*, 12, 1479–1498, <https://doi.org/10.5194/tc-12-1479-2018>, 2018.
- 750 Wilson, E.A., Riser, S. C., Campbell, E. C., and Wong, A. P. S.: Winter upper-ocean stability and ice–ocean feedbacks in the sea ice–covered Southern Ocean, *J. Phys. Ocean.*, 49, 1099–1117, <https://doi.org/10.1175/JPO-D-18-0184.1>, 2019.
- Weijer, W., Veneziani, M., Stössel, A., Hecht, M. W., Jeffery, N., Jonko, A., Hodos, T., and Wang, H.: Local atmospheric response to an open-ocean polynya in a high-resolution climate model, *J. Clim.*, 30, 1629–1641, <https://doi.org/10.1175/JCLI-D-16-0120.1>, 2017.
- 755 Zanoski, H., Hallberg, R., and Sarmiento, J. L.: Abyssal ocean warming and salinification after Weddell Polynyas in the GFDL CM2G coupled climate model, *J. Phys. Oceanogr.*, 45, 2755–2772, <https://doi.org/10.1175/JPO-D-15-0109.1>, 2015.
- Zhang L., Delworth, T. L., Cooke, W., and Yang, X.: Natural variability of Southern Ocean convection as a driver of observed climate trends, *Nat. Clim Change*, 9, 59–65, <https://doi.org/10.1038/s41558-018-0350-3>, 2019.
- Zhang L., Delworth, T. L., Cooke, W., Goosse, H., Mitchell, B., Morioka, Y., and Yang, X.: On the mean state dependence of
760 Southern Ocean low frequency internal variability, *J. Clim.* (submitted), 2020.
- Zhao, M., Golaz, J.-C., Held, I. M., Guo, H., Balaji, V., Benson, R., Chen, J.-H., Chen, X., Donner, L. J., Dunne, J. P., Dunne, K. A., Durachta, J., Fan, S.-M., Freidenreich, S. M., Garner, S. T., Ginoux, P., Harris, L. M., Horowitz, L. W., Krasting, J. P., Langenhorst, A. R., Liang, Z., Lin, P., Lin, S.-J., Malyshev, S., Mason, E., Milly, P.C.D., Ming, Y., Naik, V., Paulot, F., Paynter, D., Phillipps, P., Radhakrishnan, A., Ramaswamy, V., Robinson, T., Schwarzkopf, D., Seman, C. J., Shevliakova, E.,
765 Shen, Z., Shin, H., Silvers, L., Wilson, J. R., Winton, M., Wittenberg, A. T., Wyman, B., and Xiang, B.: The GFDL global



atmosphere and land model AM4.0/LM4.0: 2. Model description, sensitivity studies, and tuning strategies, *J. Adv. Model. Earth Syst.*, 10, 735–769, <https://doi.org/10.1002/2017MS001209>, 2018.

Zwally, H. J., Comiso, J. C., Parkinson, C. L., Campbell, W. J., Carsey, F. D., and Gloersen, P.: Antarctic sea ice, 1973–1976: Satellite passive-microwave observations, *NASA Spec. Publ.*, SP-459, 206 pp.

770 <https://ntrs.nasa.gov/archive/nasa/casi.ntrs.nasa.gov/19840002650.pdf>, 1983.



775 **Table 1 –Ice-core records used in this study (based on Medley and Thomas, 2019 and Stenni et al., 2017). The surface mass balance from the first 6 records are used in the reconstructions of the polynya activity. The other records (*in italic*) are only displayed on Figs. 2 and 3.**

Number	Site name	Longitude (°)	Latitude (°)	Altitude (m)	Years CE	Reference
1	Berkner Island (South)	-45.72	-79.57	890	1000–1992	Mulvaney et al. (2002)
2	B31Site DML07	-3.43	-75.58	2680	1000–1994	Graf W. et al. (2002)
3	B32Site DML05	-0.01	-75.00	2892	1248–1996	Graf W. et al. (2002) Sommer et al. (2000) Oerter et al. (2000)
4	B40	0.07	-75.00	2892	1–2010	Medley et al. (2018)
5	Fimbulisen S100	4.8	-70.24	48	1737–1999	Kaczmarska et al. (2004)
6	B33Site DML17	6.5	-75.17	3160	1250–1997	Graf W. et al. (2002) Sommer et al. (2000) Oerter et al. (2000)
7	<i>Derwael Ice Rise IC12</i>	<i>26.34</i>	<i>-70.25</i>	<i>450</i>	<i>1744–2011</i>	<i>Phillipe et al. (2016)</i>
8	<i>H72</i>	<i>41.08</i>	<i>-69.2</i>	<i>1214</i>	<i>1832–1999</i>	<i>Nishio et al. (2002)</i>
9	<i>IND 22B4</i>	<i>11.54</i>	<i>-70.86</i>	<i>500</i>	<i>1533–1994</i>	<i>Laluraj et al. (2011)</i>
11	<i>NUS 08-7</i>	<i>1.6</i>	<i>-74.12</i>	<i>2673</i>	<i>1382–2008</i>	<i>Steig et al. (2013)</i>
12	<i>NUS 07-1</i>	<i>7.94</i>	<i>-73.72</i>	<i>3174</i>	<i>1706–2005</i>	<i>Steig et al. (2013)</i>



780

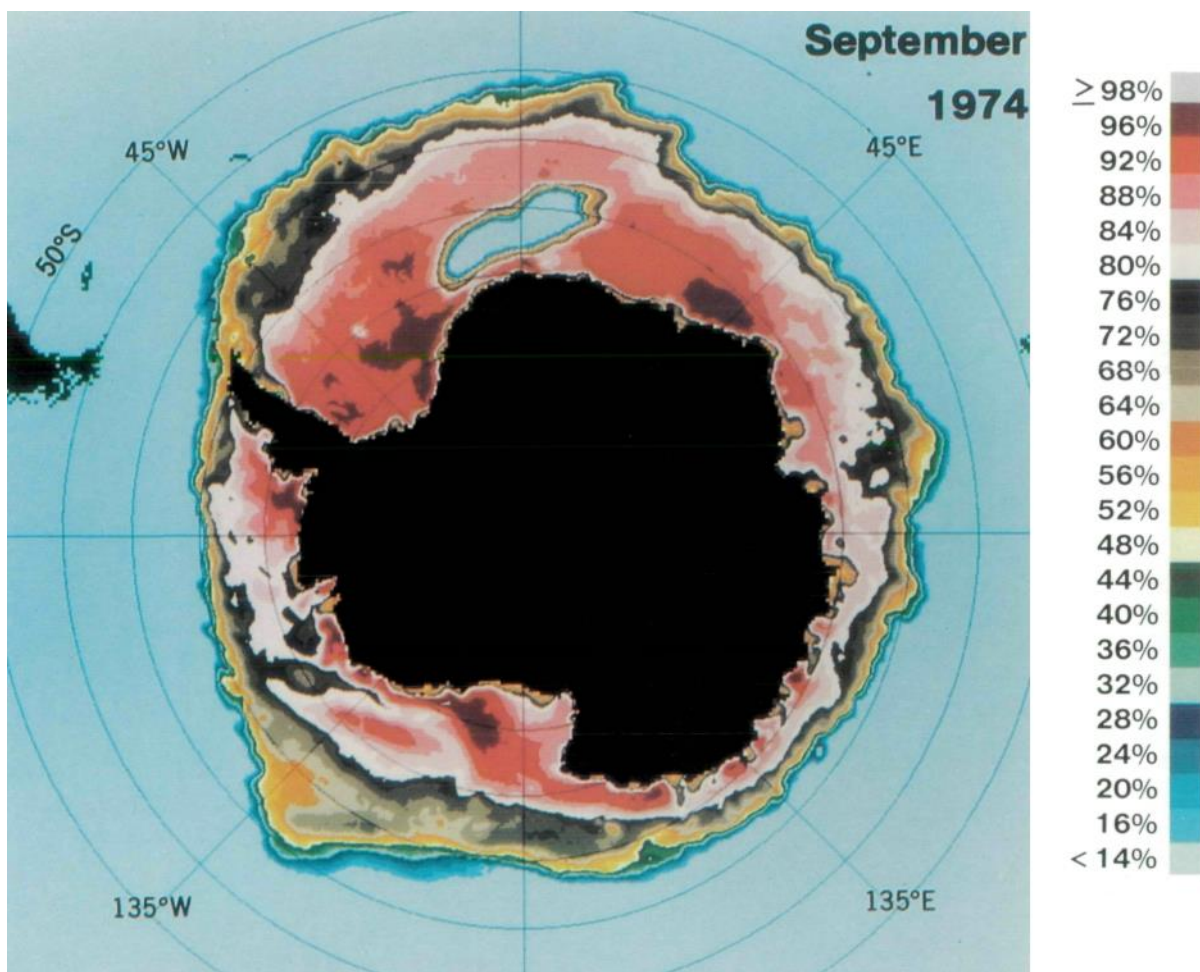
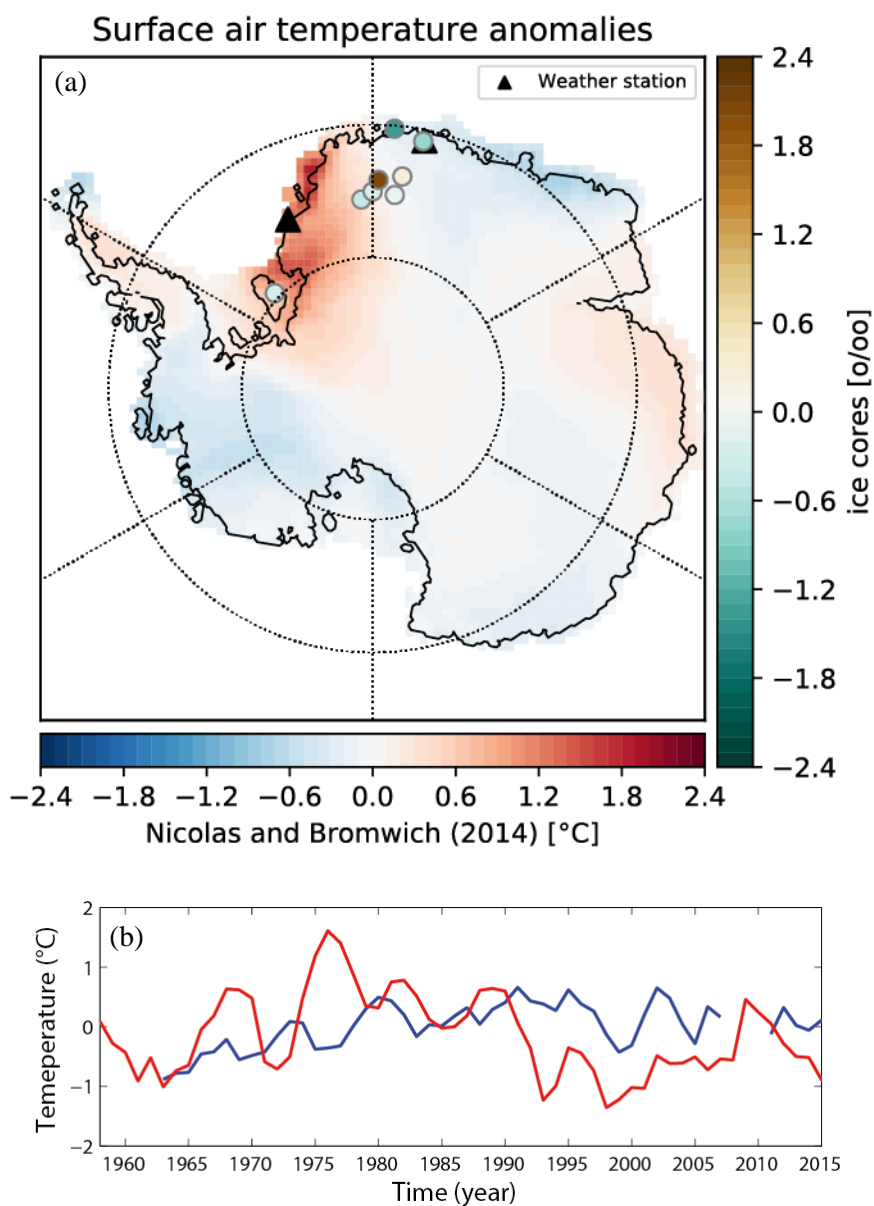


Figure 1: The Weddell Sea polynya in Austral winter, September 1974. Violet and red correspond to a high sea ice concentration and light blue to open ocean. The Weddell Sea polynya is visible across the Greenwich meridian. Figure from Zwally et al. (1983).

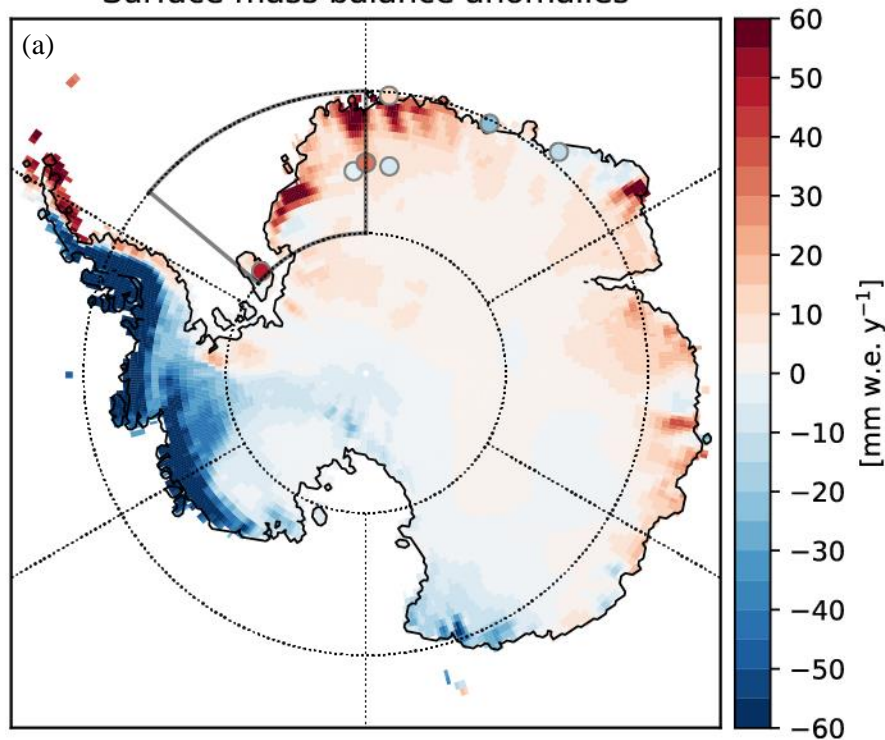
785



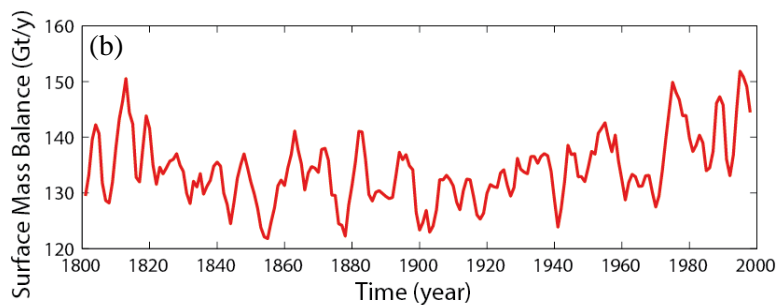
790 **Figure 2:** a) Annual mean temperature anomaly (°C) averaged over 1974-1976 compared to the period 1958-2000 in the Nicolas and Bromwich (2014a) reconstruction. The dots correspond to the $\delta^{18}\text{O}$ (‰) anomalies for the same period in ice cores in the region of interest. b) Annual mean temperature anomaly (°C) at Halley (red) and Novolazarevskaya (blue) weather stations. A 3-year running mean has been applied to the series.



Surface mass balance anomalies

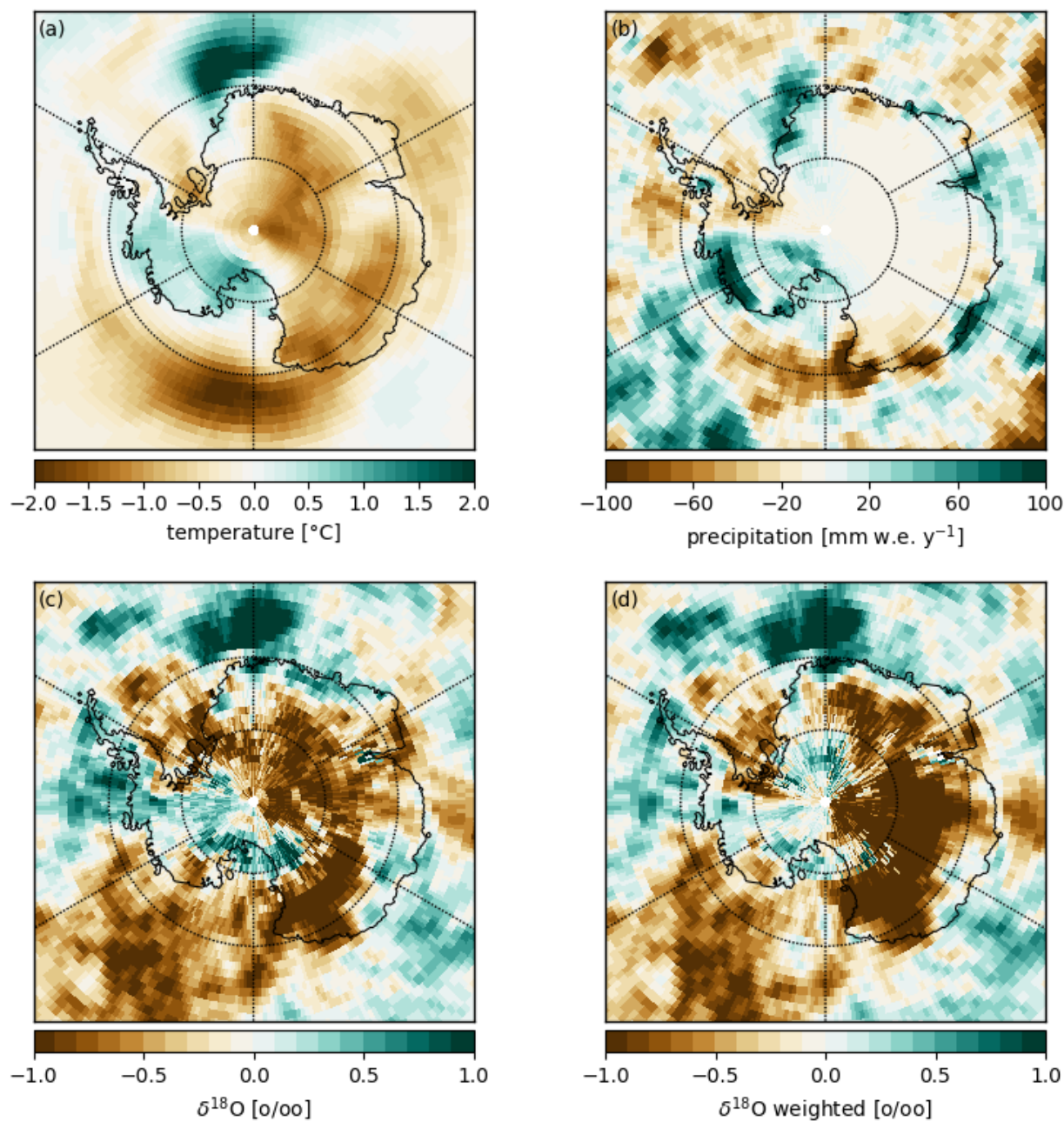


795

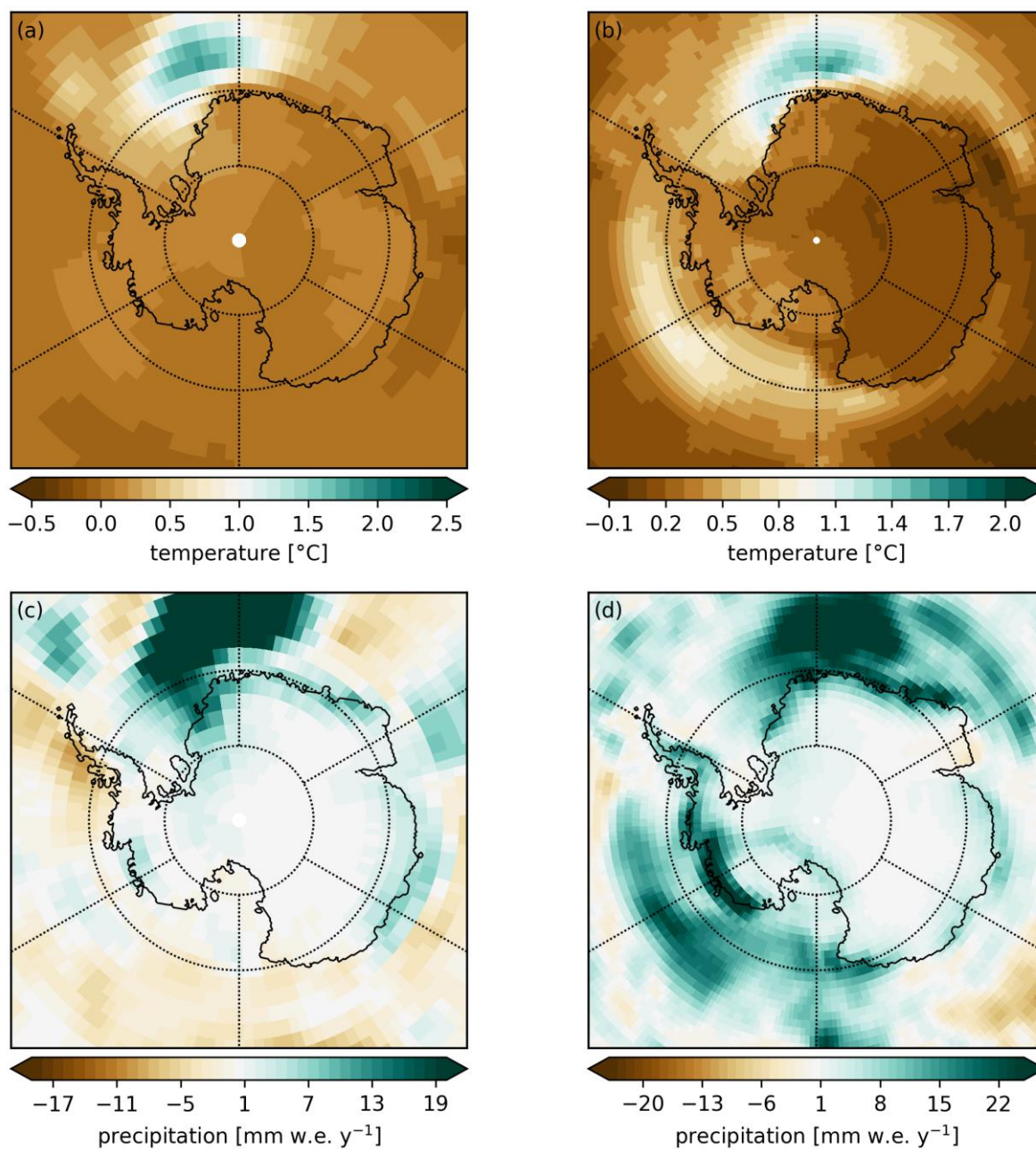


800

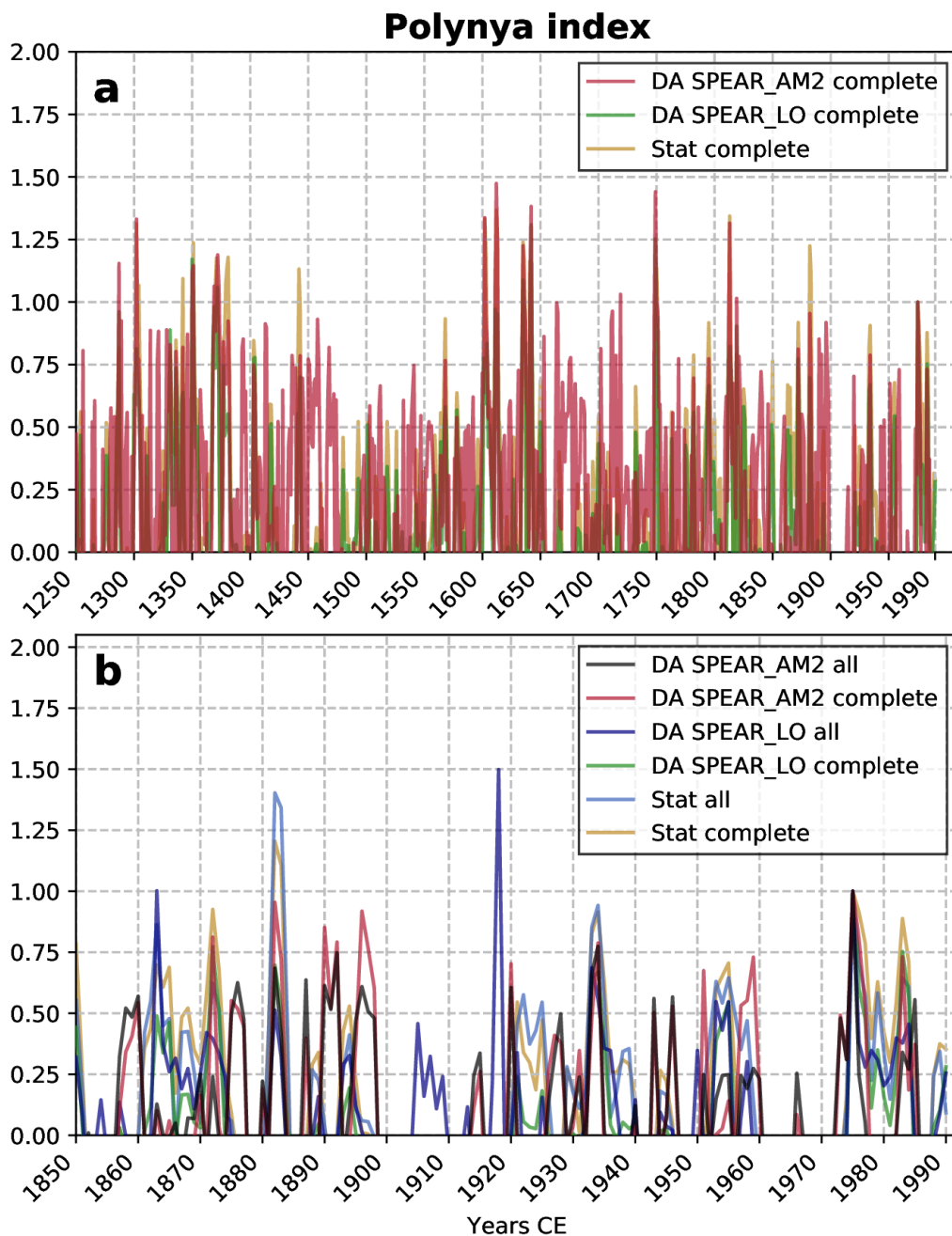
Figure 3: a) Anomaly of SMB (mm w.e. /y) averaged over 1974-1976 compared to the period 1958-2000 in the Medley and Thomas (2019) reconstruction. The dots correspond to the estimates from the ice cores selected in the reconstruction for the region of interest. b) SMB (Gt/y) integrated over the grounded ice sheet between 50 W 0°E, north of 80°S (box on panel a) in Medley and Thomas (2019) reconstruction. A 3-year running mean has been applied to the series.



805 **Figure 4: Anomaly of (a) annual mean temperature (°C), (b) precipitation (mm w.e./y), (c) mean $\delta^{18}\text{O}$ of precipitation (ppm) and (d) mean $\delta^{18}\text{O}$ weighted by the precipitation amount averaged over 1974-1976 compared to the period 1958-2000 in a simulation performed with ECHAM5-wiso (ppm).**



810 **Figure 5:** (a) Regression of annual mean temperature (°C) and (c) precipitation (mm w.e. /y) scaled to correspond to one standard deviation change of the annual mean ocean mixed layer depth in the Eastern Weddell Sea between -50°W and 50°E, southward of 60°S over the years 2000-3000 of the SPEAR_AM2 simulation. Same in (b, d) for the years 3000-4000 of the SPEAR_LO simulation.



815

820

Figure 6: a) Index of polynya activity based on 5 surface mass balance records using a simple average of standardized time series (Stat complete, orange), data assimilation with SPEAR-LO (DA SPEAR_LO complete, green) and SPEAR AM2 (DA SPEAR_AM2 complete, red) as priors for the years 1250-1992 and b) for the years 1850-2000. The panel (b) also includes the index of polynya activity based on 6 surface mass balance records using the same methods (Stat all in light blue, DA SPEAR_LO all in dark blue, DA SPEAR_AM2 all in black). The times series have all been scaled to have a value of 1 in 1975.



Percentage of time with polynya

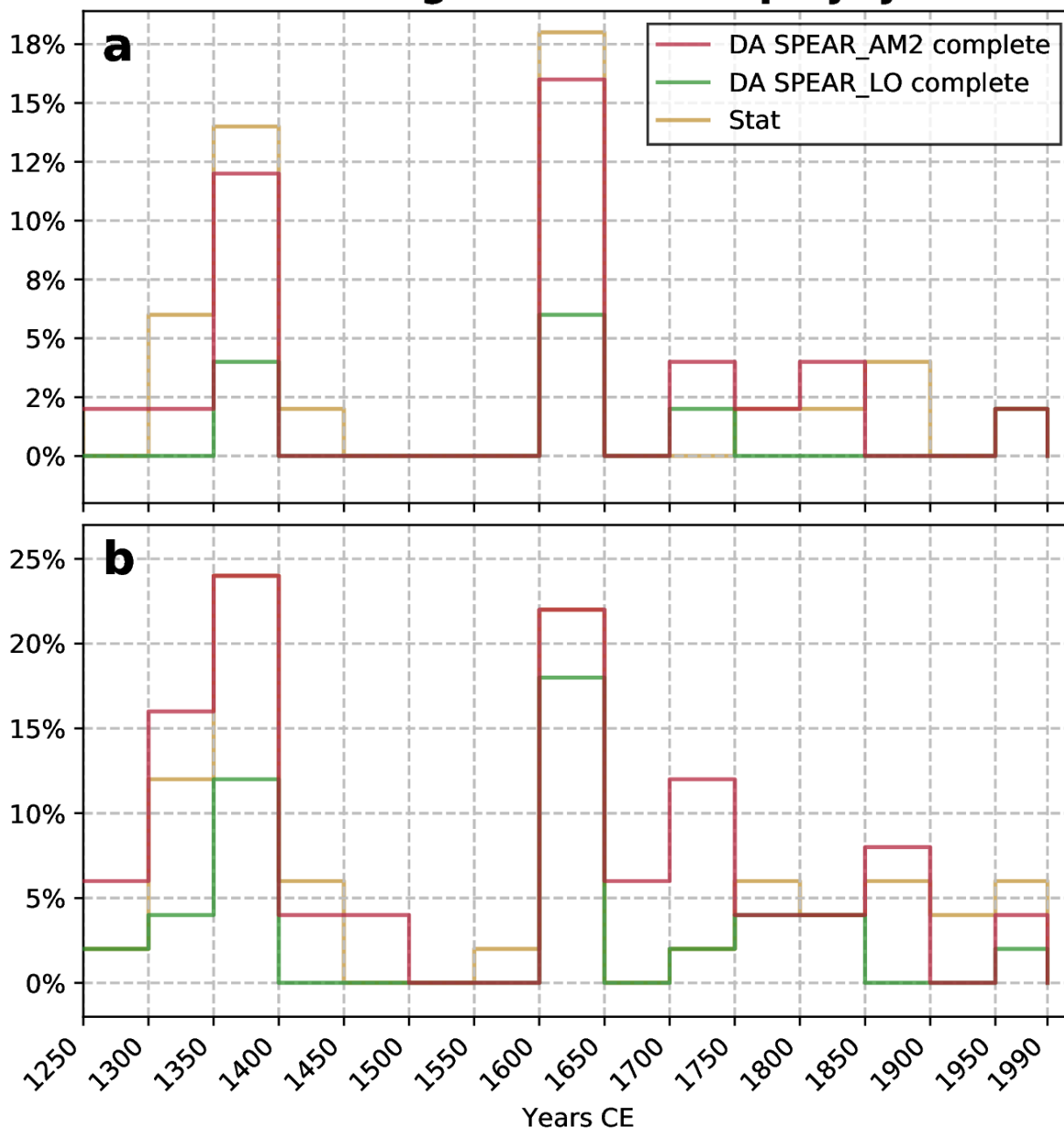


Figure 7: Percentage of the years with the index of polynya activity higher than 1 (a) and 0.8 (b) per 50 year time interval in the reconstructions based on 5 surface mass balance records using a simple average of standardized time series (Stat complete, orange), data assimilation with SPEAR-LO (DA SPEAR_LO complete, green) and SPEAR AM2 (DA SPEAR_AM2 complete, red) as priors.

825